



Nucleon tomography in the threshold limit

Ding-Yu Shao
Fudan University

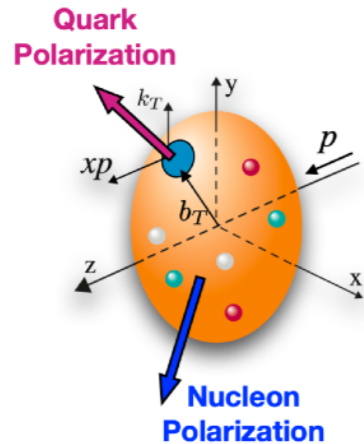
Heavy Ion Physics in the EIC Era

INT (Seattle)

Aug 22 2024

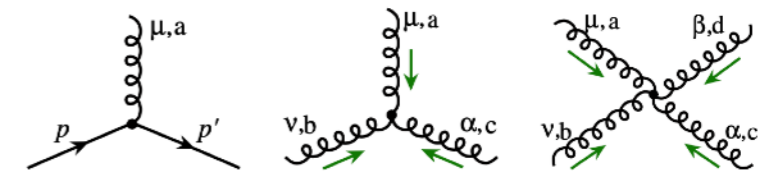
Introduction

Transverse momentum distributions (TMDs) encode the quantum correlations between hadron polarization and the motion and polarization of quarks and gluons inside it.



Imaging a hadron would provide insights on QCD

$$-\frac{1}{4}G_{\mu\nu,a}^2[A] + \sum_f \bar{\psi}_f (iD_\mu[A]\gamma^\mu - m_f) \psi_f$$



- Both longitudinal and transverse motion
- Large Lorentz boost in longitudinal direction, but not in transverse momentum
- Correlation between hadron **spin** with parton(quark, gluon) **orbital angular momentum**

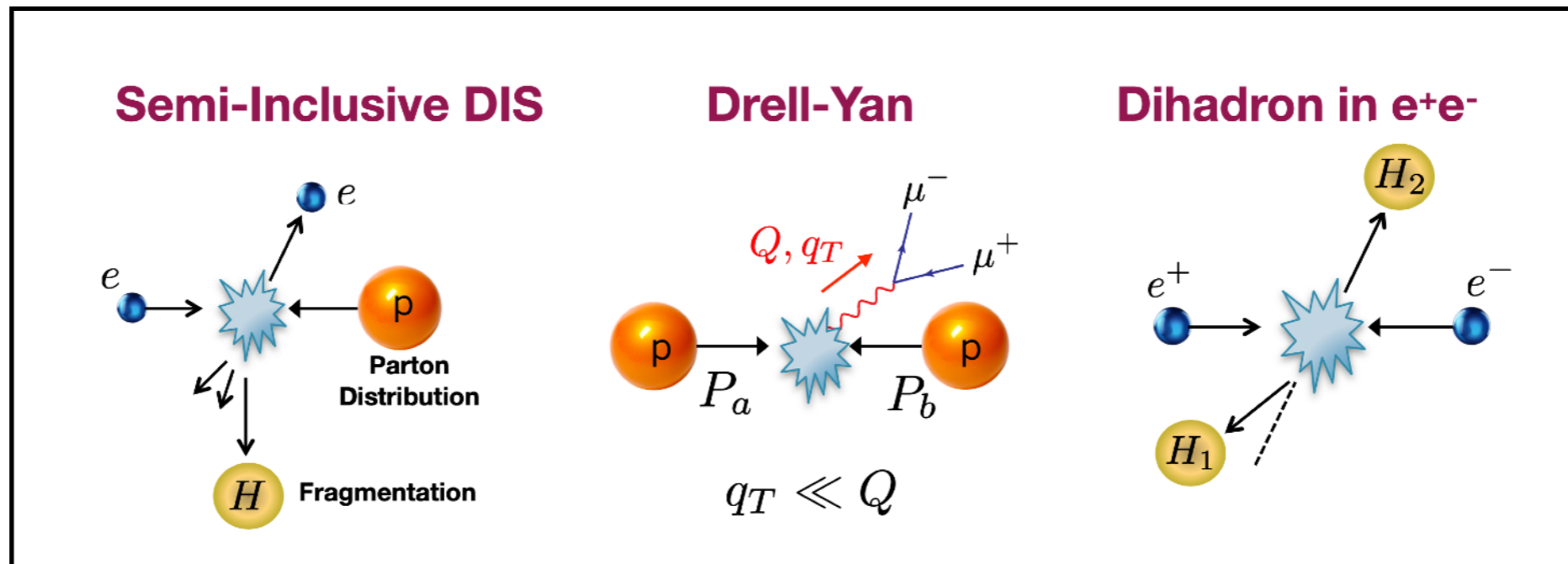
TMDs		Quark Polarization		
		Unpolarized (U)	Longitudinally polarized (L)	Transversely polarized (T)
Nucleon Polarization	U	f_1 unpolarized		h_1^\perp Boer-Mulders
	L		g_{1L} helicity	h_{1L}^\perp longi-transversity
	T	f_{1T}^\perp Sivers	g_{1T} trans-helicity	h_1 transversity h_{1T}^\perp pretzelosity

○ → Nucleon spin ● → Quark spin

Figure 2.5: The leading-twist quark TMD distributions.

Transverse momentum distributions of quarks

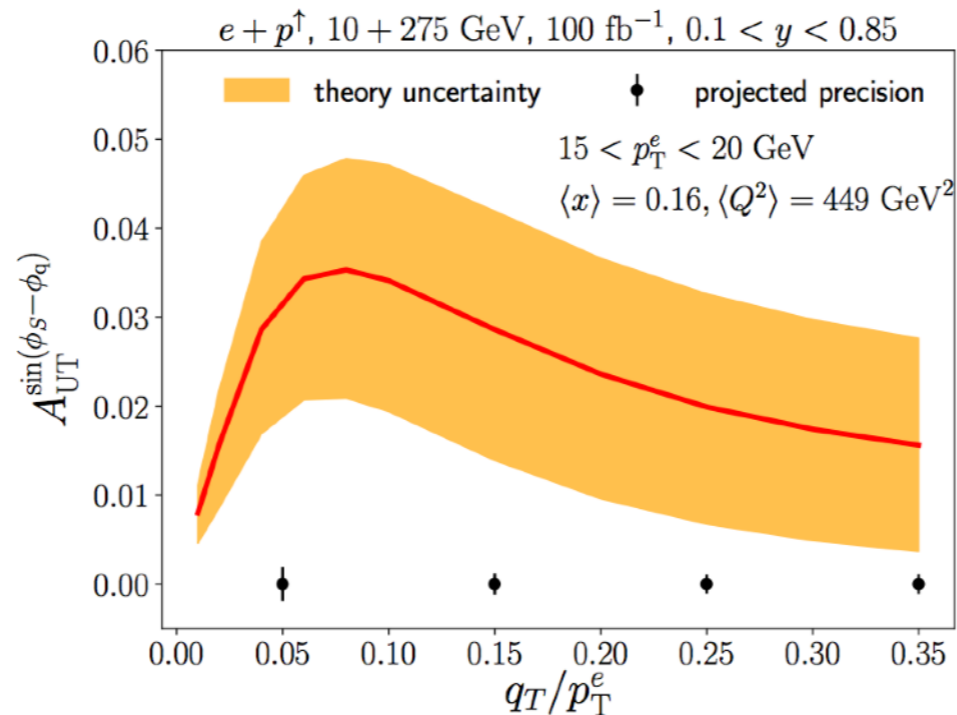
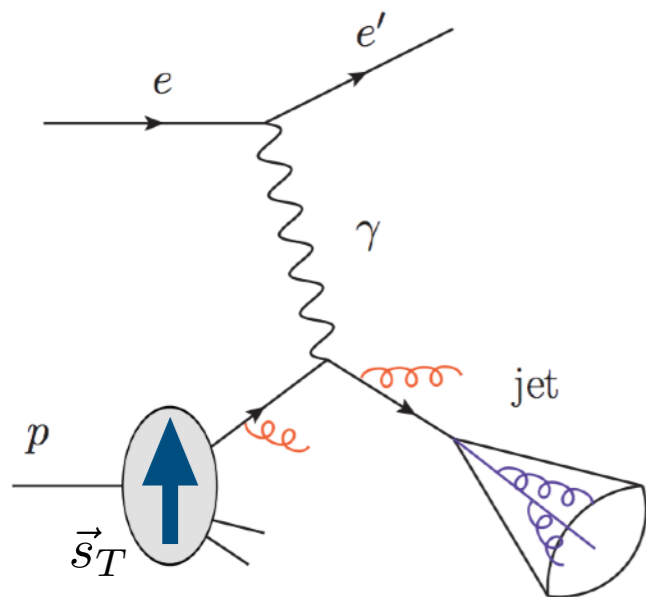
- Three classical processes used to probe quark TMDs



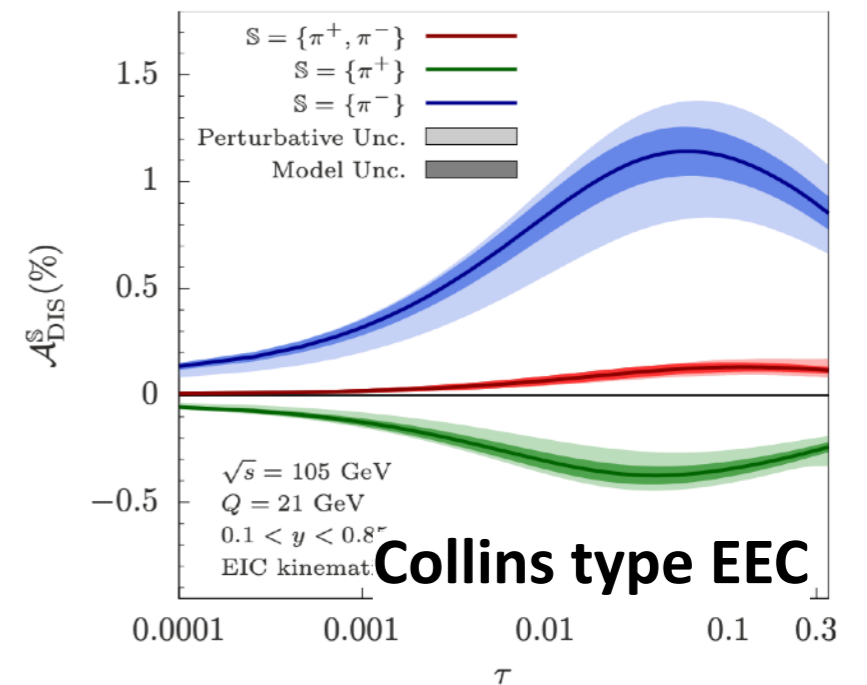
- Typical “two-scale” problem:
transverse momentum of final particle (q_T) \ll scattering energy (Q)
- Theory tools: TMD factorization theorem, effective field theory Collins-Soper-Sterman, Ji-Ma-Yuan, Soft-Collinear Effective Theory

$$\frac{d\sigma(ep \rightarrow ehX)}{dQ dx dz d\vec{q}_T} = H_{eq \rightarrow eq}(Q) F_q(\vec{q}_T, x) \otimes D_{q \rightarrow h}(\vec{q}_T, z)$$

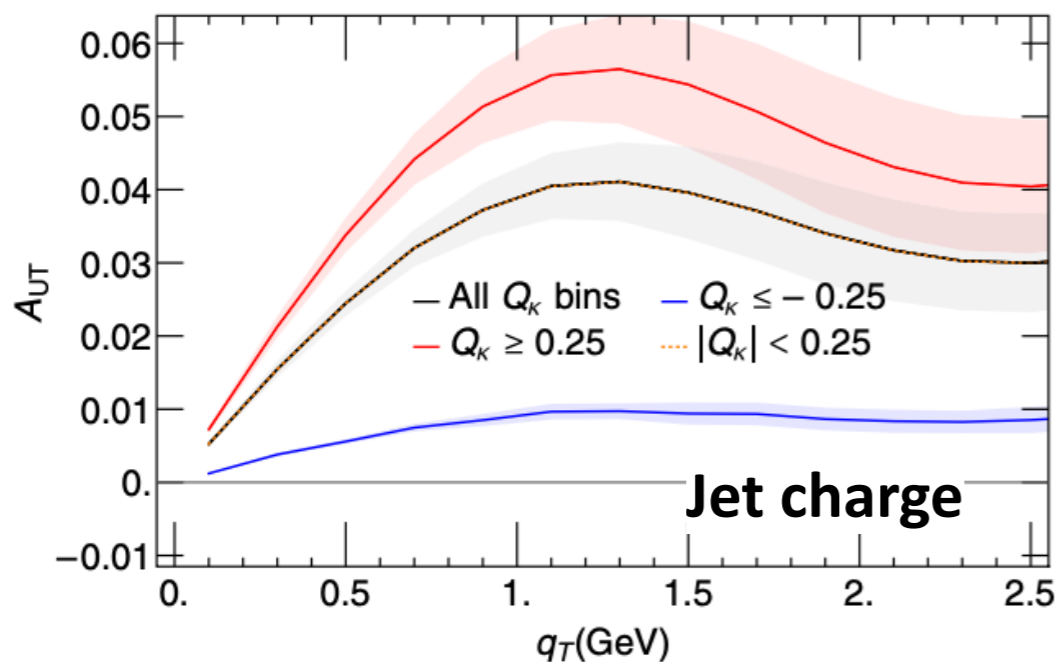
Jets and 3D imaging



Arratia, Kang, Prokudin, Ringer '19
Liu, Ringer, Vogelsang, Yuan '19



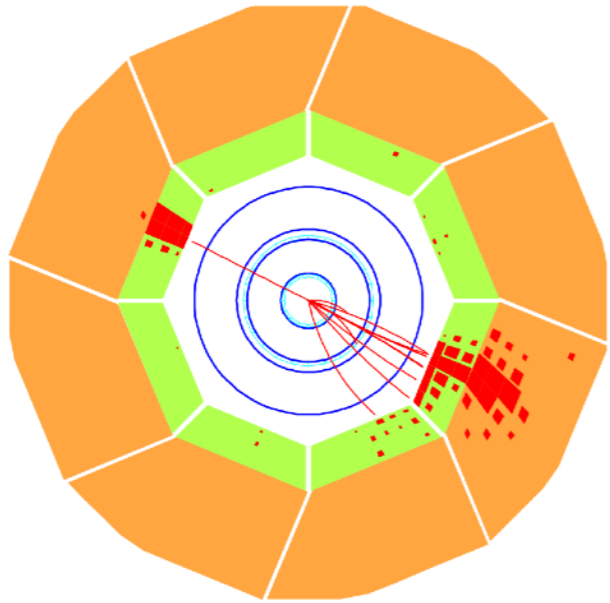
Kang, Lee, DYS, Zhao '23 JHEP



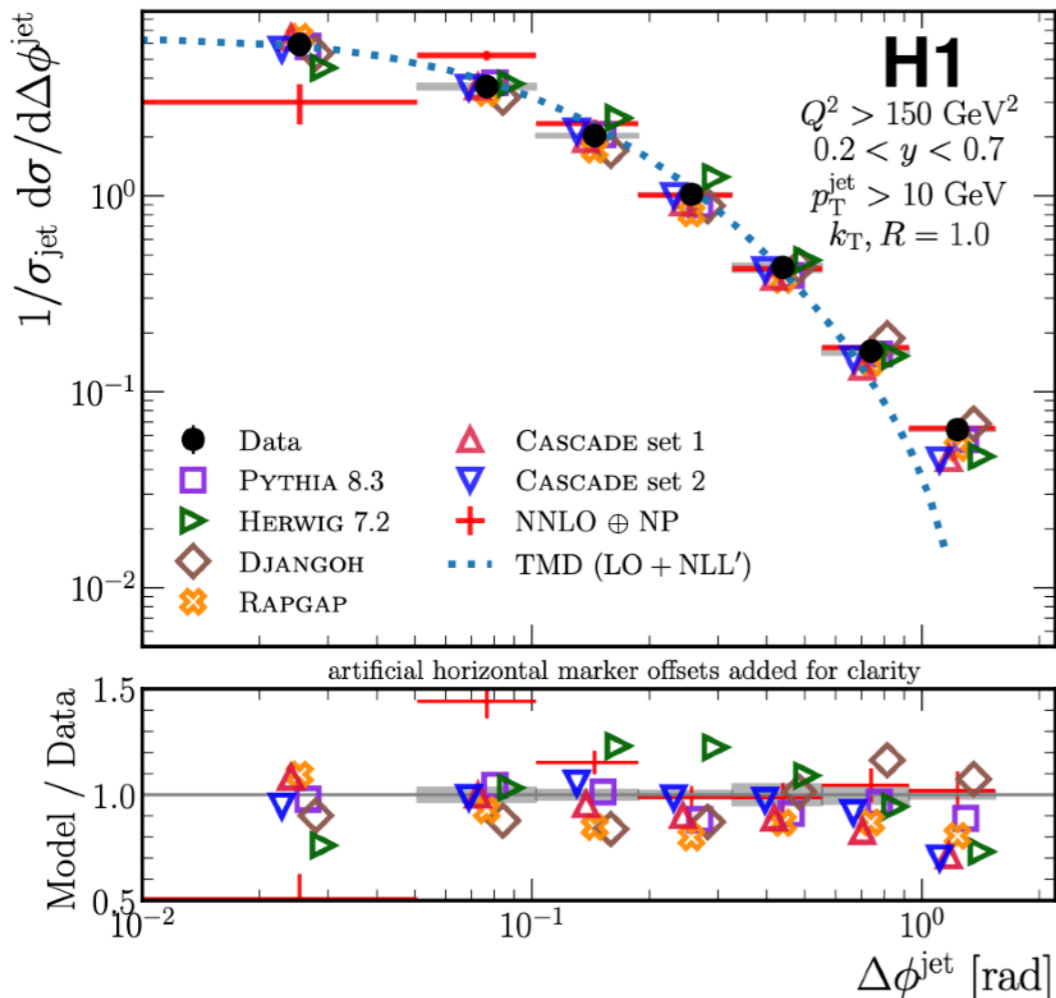
Kang, Liu, Mantry, DYS '20 PRL

- Jets are complementary to standard SIDIS extractions of TMDs
- Jet measurements allow independent constraints on TMD PDFs and FFs from a single measurement
- Azimuthal correlation between jet and lepton sensitive to TMD PDFs

Jets and 3D imaging



- NLL resummation result is consistent with HERA data
 - Open questions:
 - Higher accuracy? SIDIS is known at N3LL' accuracy
 - Better angular resolution?
 - Reduce contamination from UE?
 - One possible solution:
 - Recoil-free jet definition (Gutierrez-Reyes, Scimemi, Waalewijn, Zoppi '18 '19)
- E.g. anti- k_T clustering algorithm + p_{T^n} -weighted recombination scheme



H1 2108.12376

Recoil-free jet and all-order structure

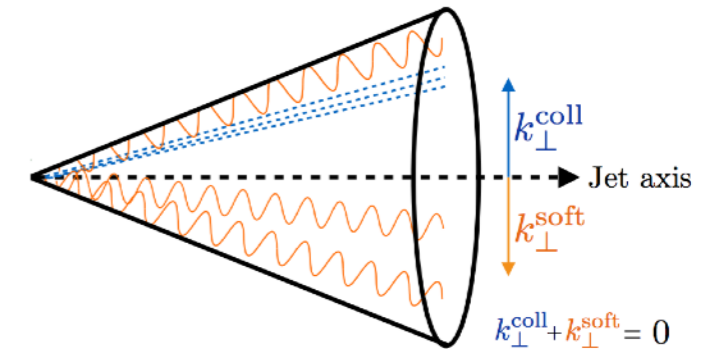
- Recoil absent for the p_T^n -weighted recombination scheme (Banfi, Dasgupta & Delenda '08)

$$p_{t,r} = p_{t,i} + p_{t,j},$$

$$\phi_r = (w_i \phi_i + w_j \phi_j) / (w_i + w_j)$$

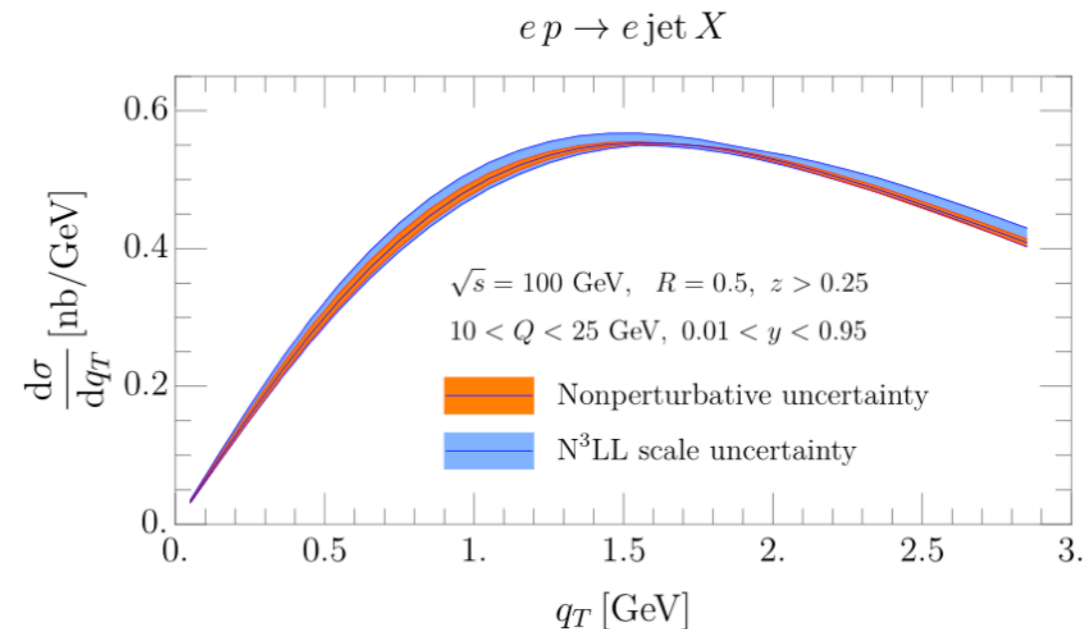
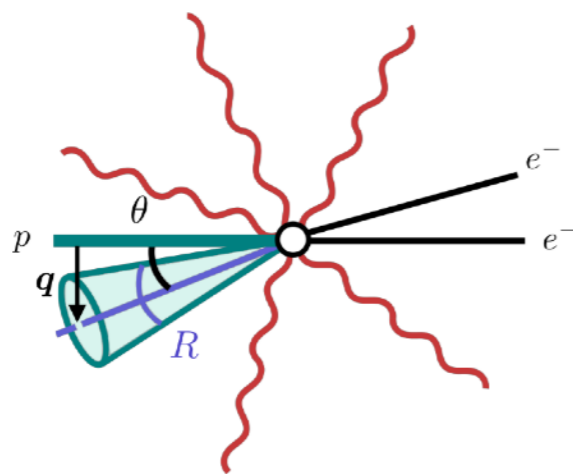
$$y_r = (w_i y_i + w_j y_j) / (w_i + w_j)$$

$$w_i = p_t^n$$



$n \rightarrow \infty$ Winner-take-all scheme (Bertolini, Chan, Thaler '13)

- N3LL resummation for jet q_T @ ee and ep (Gutierrez-Reyes, Scimemi, Waalewijn, Zoppi '18 '19)



- NNLL resummation for $\delta\phi$ @ pp (Chien, Rahn, DYS, Waalewijn & Wu '22 JHEP + Schrignder '21 PLB)
- NNLL resummation for $\delta\phi$ @ ep & eA (Fang, Ke, DYS, Terry '23 JHEP)

Recoil-free azimuthal angle for electron-jet correlation

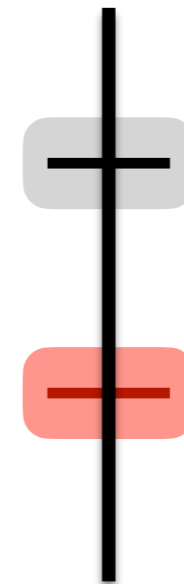
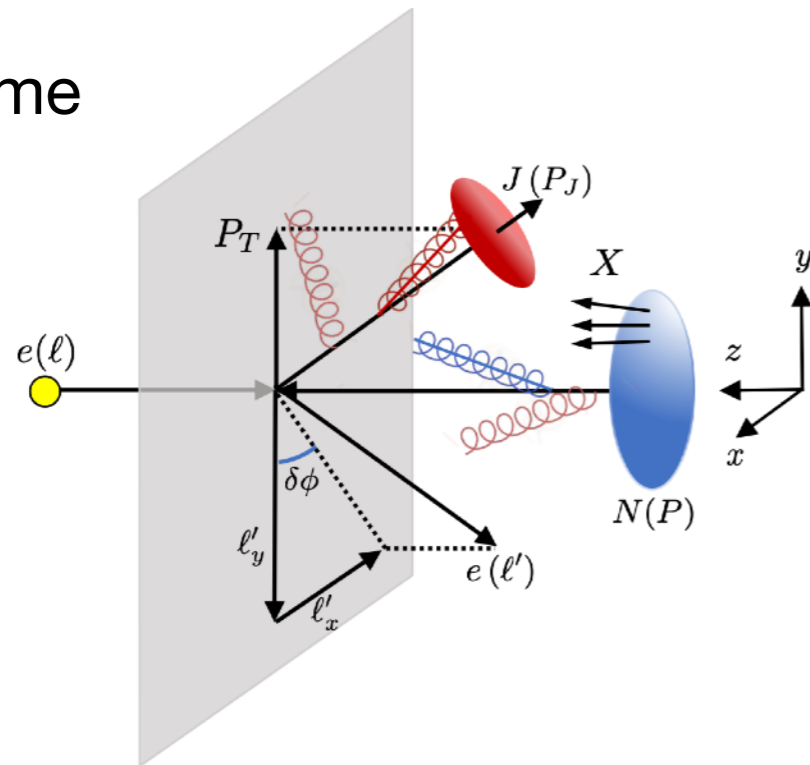
Fang, Ke, DYS, Terry '23 JHEP

$$e(\ell) + N(P) \rightarrow e(\ell') + J(P_J) + X$$

Standard TMD in back to back limit: $Q \gg q_T \sim l_T \delta\phi$

Chien, Rahn, DYS, Waalewijn & Wu '22 JHEP + Schrignder '21 PLB

Lab frame



$$p_h \sim Q(1, 1, 1)$$

$$p_{e_i}^\mu \sim l_T (\delta\phi^2, 1, \delta\phi)_{n_i \bar{n}_i}$$

$$p_s^\mu \sim l_T (\delta\phi, \delta\phi, \delta\phi)$$

Similar to Transverse-EEC in back to back

Following the standard steps in SCET and CSS, we obtain the following resummation formula

$$\frac{d\sigma}{d^2\ell'_T dy d\delta\phi} = \frac{\sigma_0 \ell'_T}{1-y} H(Q, \mu) \int_0^\infty \frac{db}{\pi} \cos(b\ell'_T \delta\phi) \sum_q e_q^2 f_{q/N}(x_B, b, \mu, \zeta_f) J_q(b, \mu, \zeta_J)$$

Hard factor

Fourier transformation
in 1-dim

TMD PDF

Jet function

Predictions in e-p

Fang, Ke, DYS, Terry '23 JHEP

TMD PDF (CSS treatment)

$$f_{q/N}(x_B, b, \mu, \zeta_f) = [C \otimes f]_{q/N}(x_B, b, \mu_f, \zeta_{fi}) U_{\text{NP}}^f(x_B, b, A, Q_0, \zeta_f) \times \exp \left[\int_{\mu_f}^{\mu} \frac{d\mu'}{\mu'} \gamma_{\mu}^f(\mu', \zeta_f) \right] \left(\frac{\zeta_f}{\zeta_{fi}} \right)^{\frac{1}{2} \gamma_{\zeta}^f(b, \mu_f)},$$

Jet function

$$J_q(b, \mu, \zeta_J) = J_q(b, \mu_J, \zeta_{Ji}) U_{\text{NP}}^J(b, A, Q_0, \zeta_J) \times \exp \left[\int_{\mu_J}^{\mu} \frac{d\mu'}{\mu'} \gamma_{\mu}^J(\mu', \zeta_J) \right] \left(\frac{\zeta_J}{\zeta_{Ji}} \right)^{\frac{1}{2} \gamma_{\zeta}^J(b, \mu_J)}$$

scale choice

$$\mu_H = Q, \quad \mu_f = \mu_J = \sqrt{\zeta_{fi}} = \sqrt{\zeta_{Ji}} = \mu_b = 2e^{-\gamma_E}/b$$

b*-prescription to avoid Landau pole

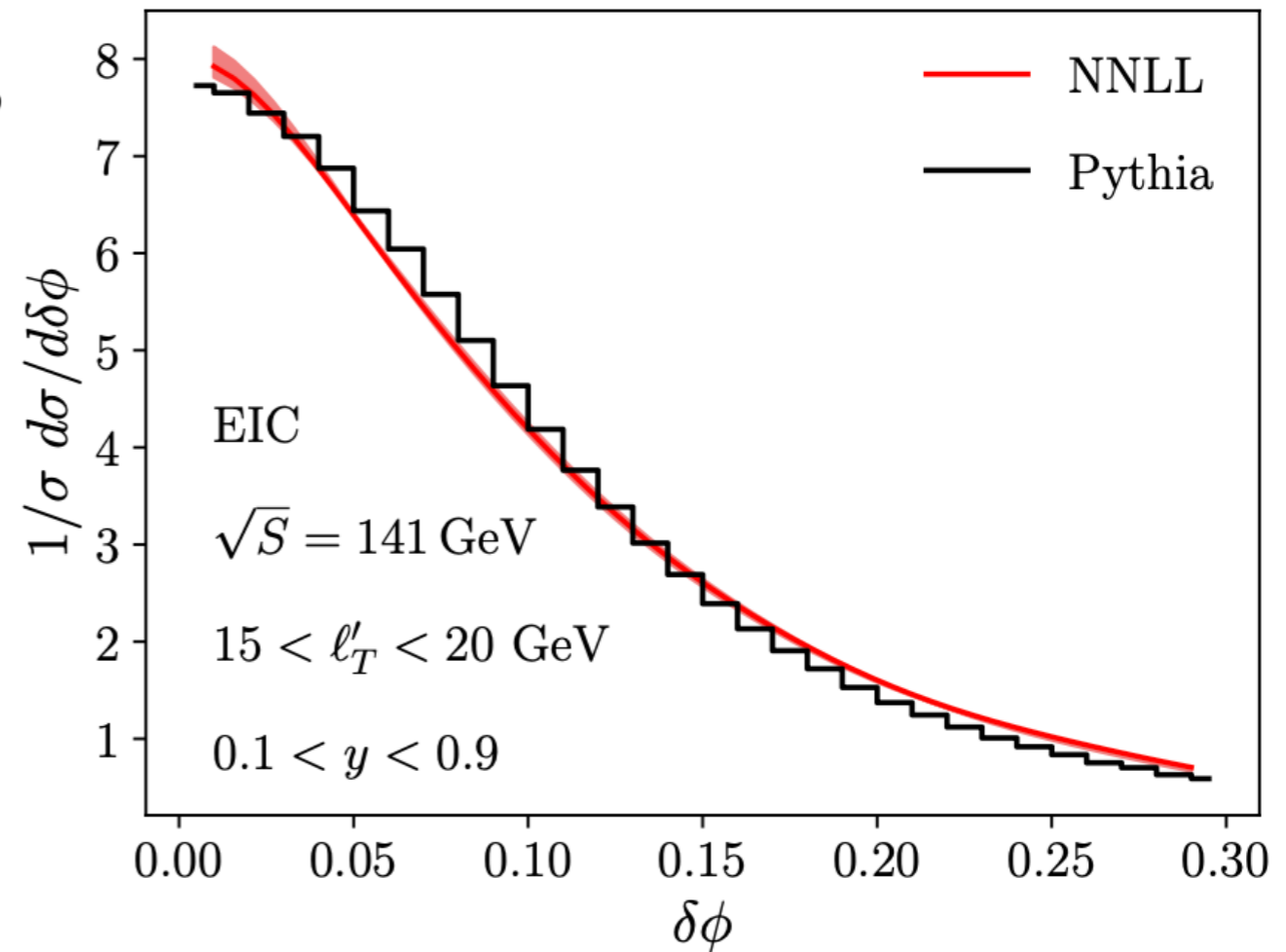
$$b_* = b / \sqrt{1 + b^2/b_{\text{max}}^2} \quad \mu_{b_*} = 2e^{-\gamma_E}/b_*$$

non-perturbative model

$$U_{\text{NP}}^f = \exp \left[-g_1^f b^2 - \frac{g_2}{2} \ln \frac{Q}{Q_0} \ln \frac{b}{b_*} \right]$$

$$U_{\text{NP}}^J = \exp \left[-\frac{g_2}{2} \ln \frac{Q}{Q_0} \ln \frac{b}{b_*} \right]$$

Sun, Isaacson, Yuan, Yuan '14



μ_H varies between $Q/2$ and $2Q$. μ_b is fixed

Predictions in e-A

Fang, Ke, DYS, Terry '23 JHEP

We apply nuclear modified TMD PDFs

$$g_1^A = g_1^f + a_N(A^{1/3} - 1) \quad a_N = 0.016 \pm 0.003 \text{ GeV}^2$$

Collinear dynamics (nPDF) using EPPS16

(Alrashed, Anderle, Kang, Terry & Xing, '22)

We include LO momentum broadening of the jet within SCET_G

$$J_q^A(b, \mu, \zeta_J) = J_q(b, \mu, \zeta_J) e^{\chi[\xi b K_1(\xi b) - 1]}$$

Opacity parameter $\chi = \frac{\rho_G L}{\xi^2} \alpha_s(\mu_{b_*}) C_F$

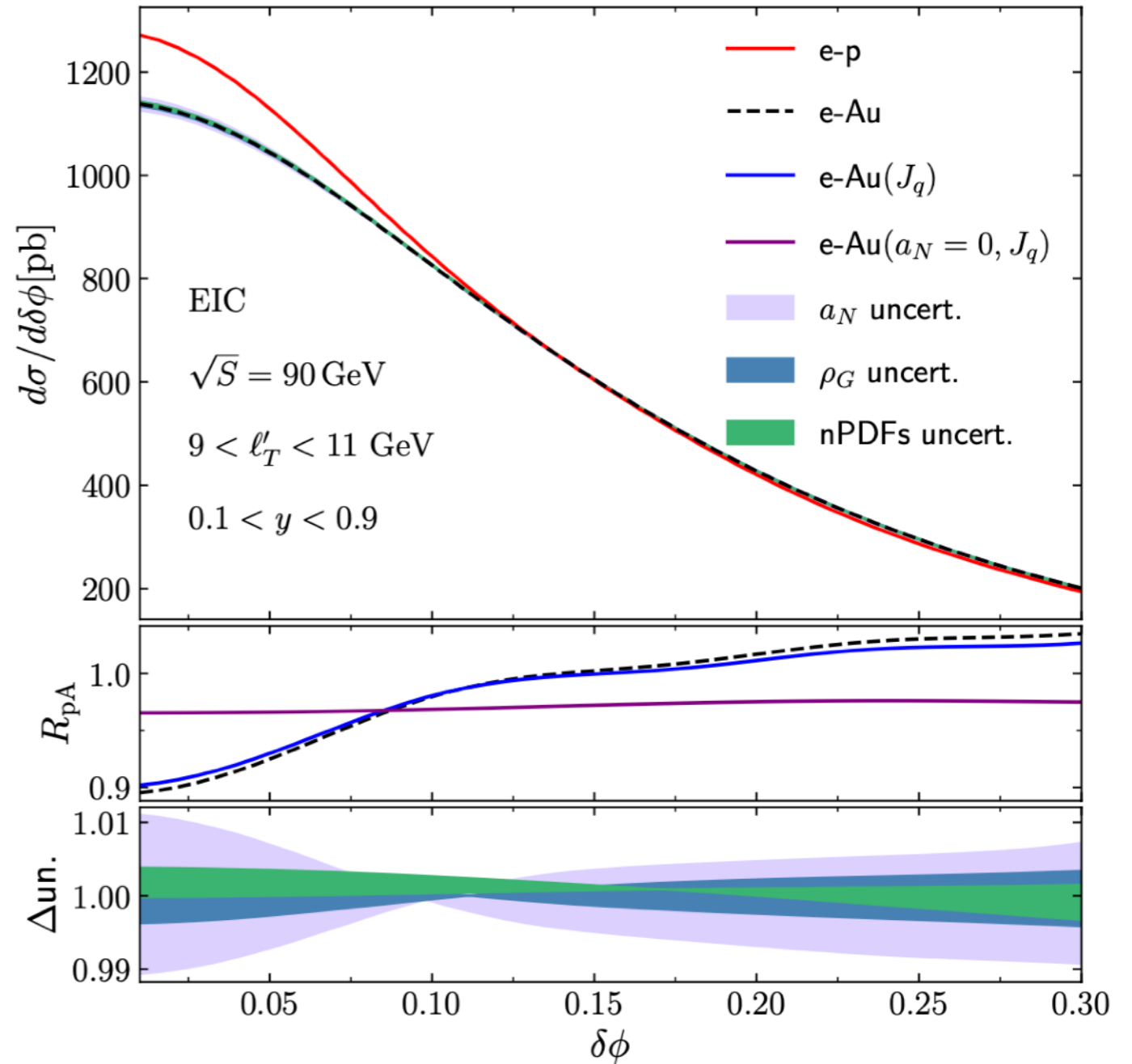
(Gyulassy, Levai, & Vitev '02)

ρ_G : density of the medium

ξ : the screening mass

L: the length of the medium

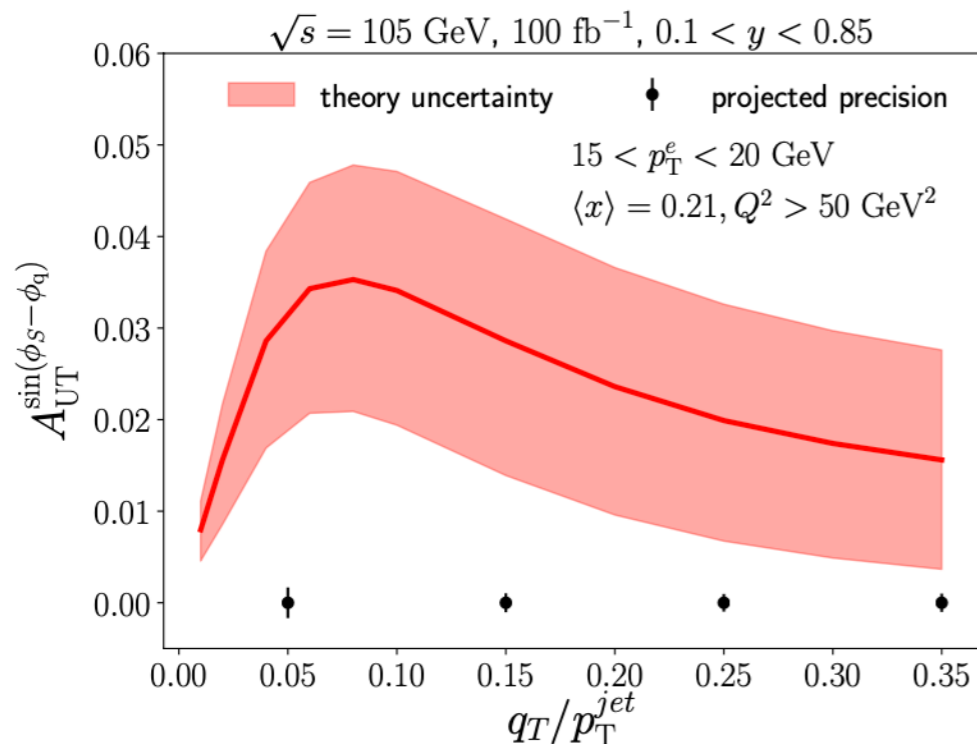
Parameter values are taken from a recent comparison between SCET_G in e-A from the HERMES Ke and Vitev '23



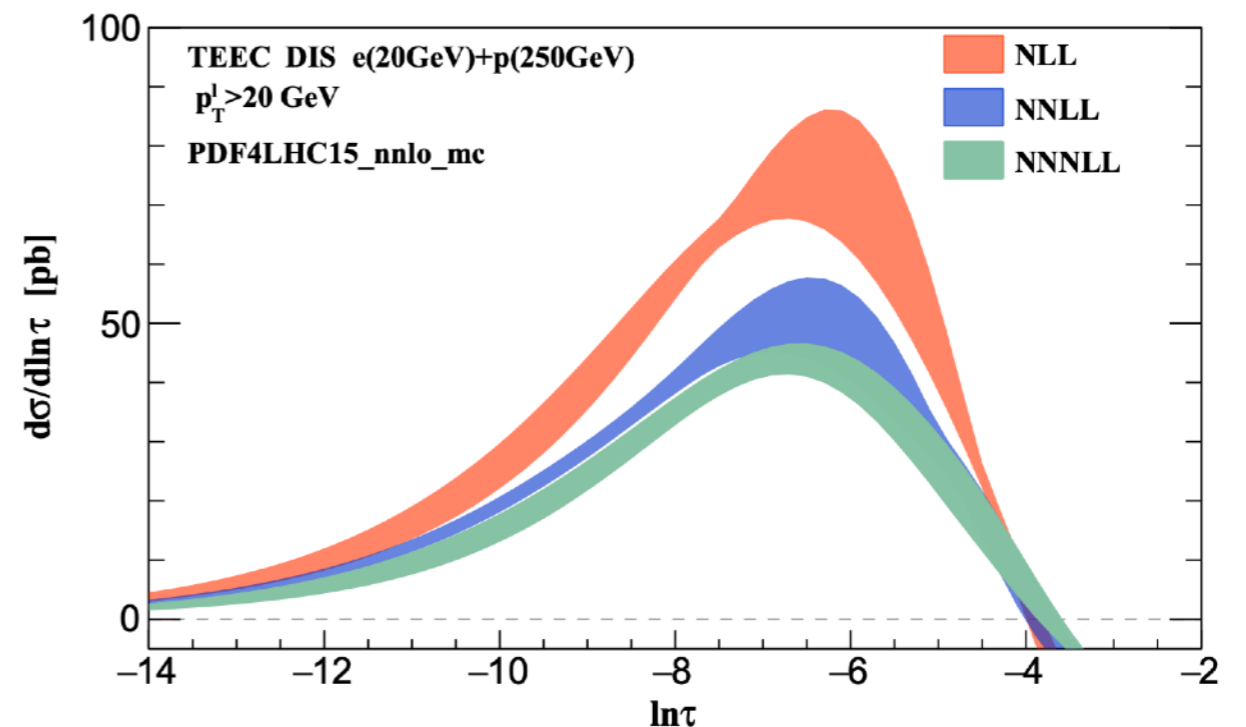
The process is primarily sensitive to the initial state's broadening effects, thereby serving as a clean probe of nTMD PDF

Precision calculation for jets in DIS

- Precision calculations in DIS are essential for enhancing our understanding of partonic interactions and the internal structure of nucleons.
- The high-order calculation has reached N3LO accuracy for jet production in DIS [Currie, Gehrmann, Glover, Huss, Niehues, & Vogt '18](#)
- Several global event shape distributions in DIS are known at N3LL + $\mathcal{O}(\alpha_s^2)$
 - **thrust** [Kang, Lee, & Stewart '15](#)
 - **(transverse) energy energy correlator** [Li, Vitev, & Zhu '20](#), [Li, Makris, Vitev '21](#)
 - **1-jettiness** [Cao, Kang, Liu & Mantry '23](#)



[Arratia, Kang, Prokudin, Ringer '19](#)



[Li, Vitev, & Zhu '20](#), [Li, Makris, Vitev '21](#)

N³LL + $\mathcal{O}(\alpha_s^2)$ predictions on lepton jet azimuthal correlation in DIS

Fang, Gao, Li, DYS 2408.XXXXX

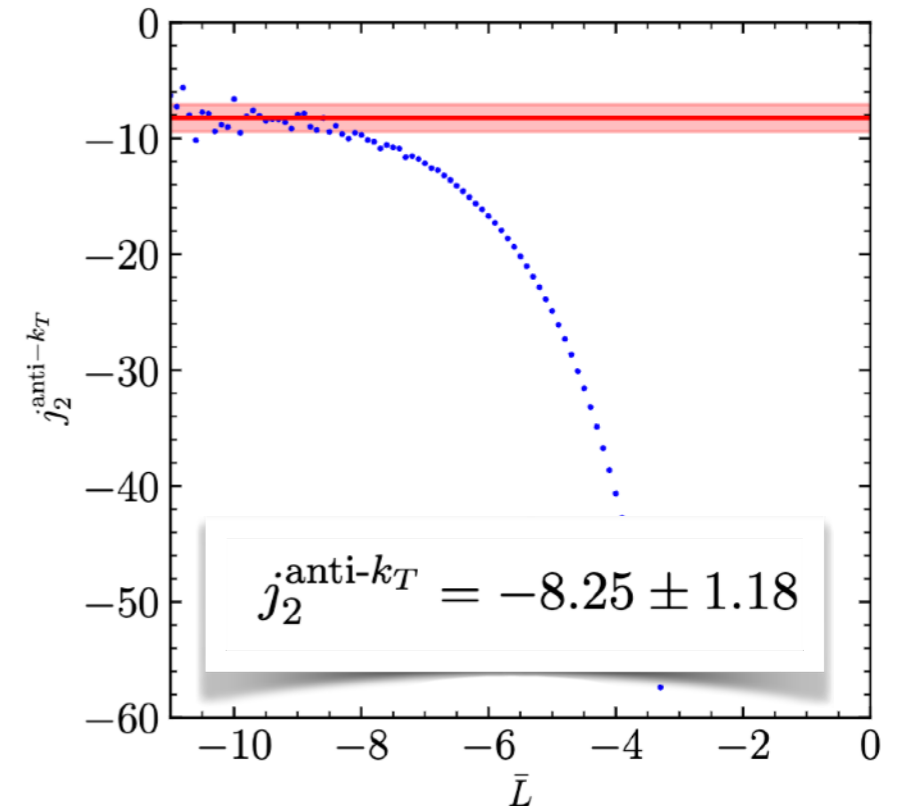
- All ingredients are known at N³LL+ $\mathcal{O}(\alpha_s^2)$, except the two loop jet function j_2 .
 - It was extracted numerically from the Event2 (Gutierrez-Reyes, Scimemi, Waalewijn, Zoppi '19)
 - A preliminary numerical results are also calculated from SoftSERVE (Brune SCET2023)
- We study dijet production in e+e-, and compare two-loop singular cross section and $\mathcal{O}(\alpha_s^2)$ predictions from NLOJET++ generator to extract j_2

$$\frac{d\sigma}{dq_T} = \bar{\sigma}_0 H(Q, \mu_h) q_T \int_0^\infty b_T db_T J_0(q_T b_T) J_q(b_T, \mu_h, \zeta_f) J_{\bar{q}}(b_T, \mu_h, \zeta_f)$$

Integrated cross section: $\sigma_L(Q_T) \equiv \int_0^{Q_T} dq_T \frac{d\sigma}{dq_T}$

Two-loop coefficient:

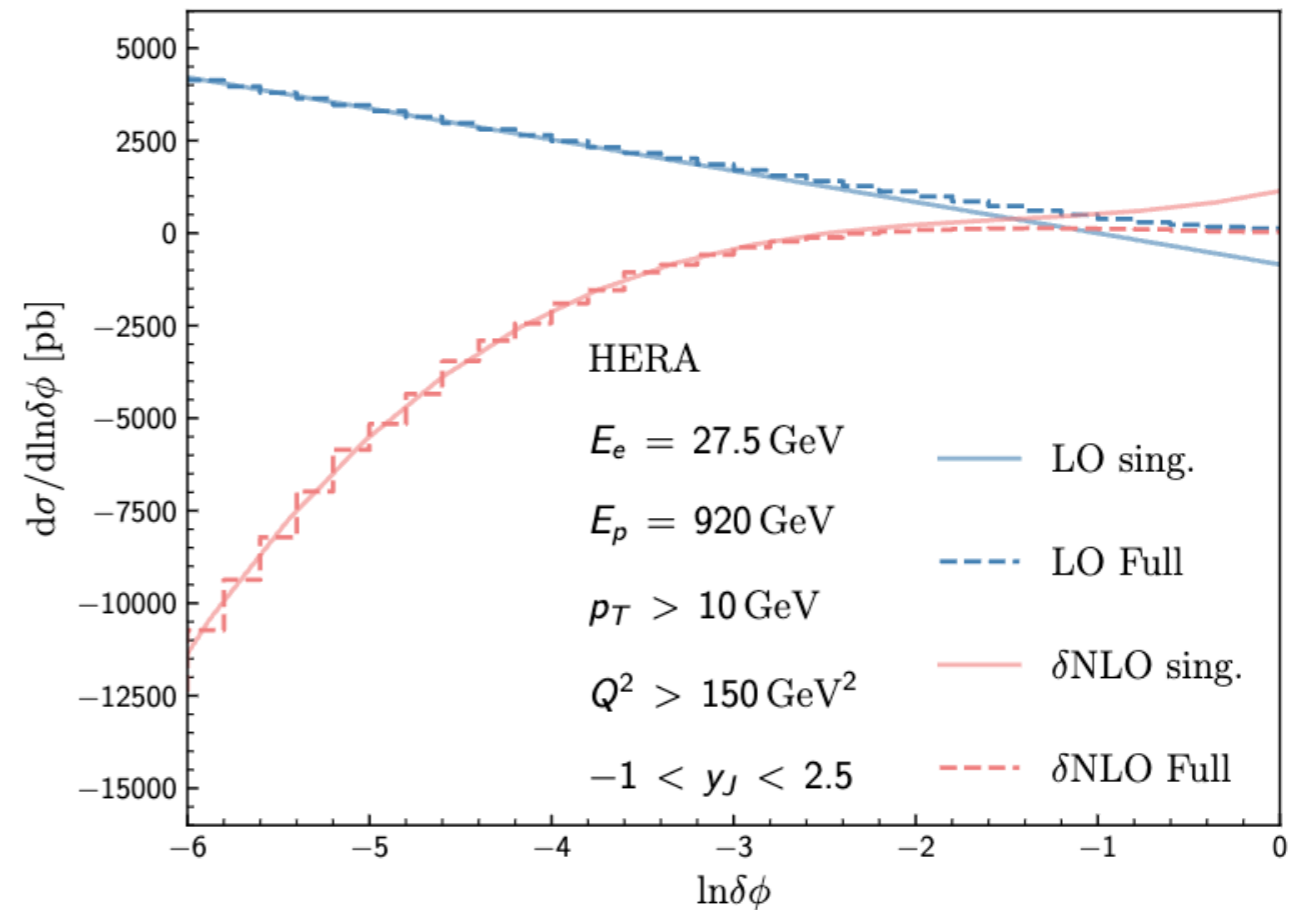
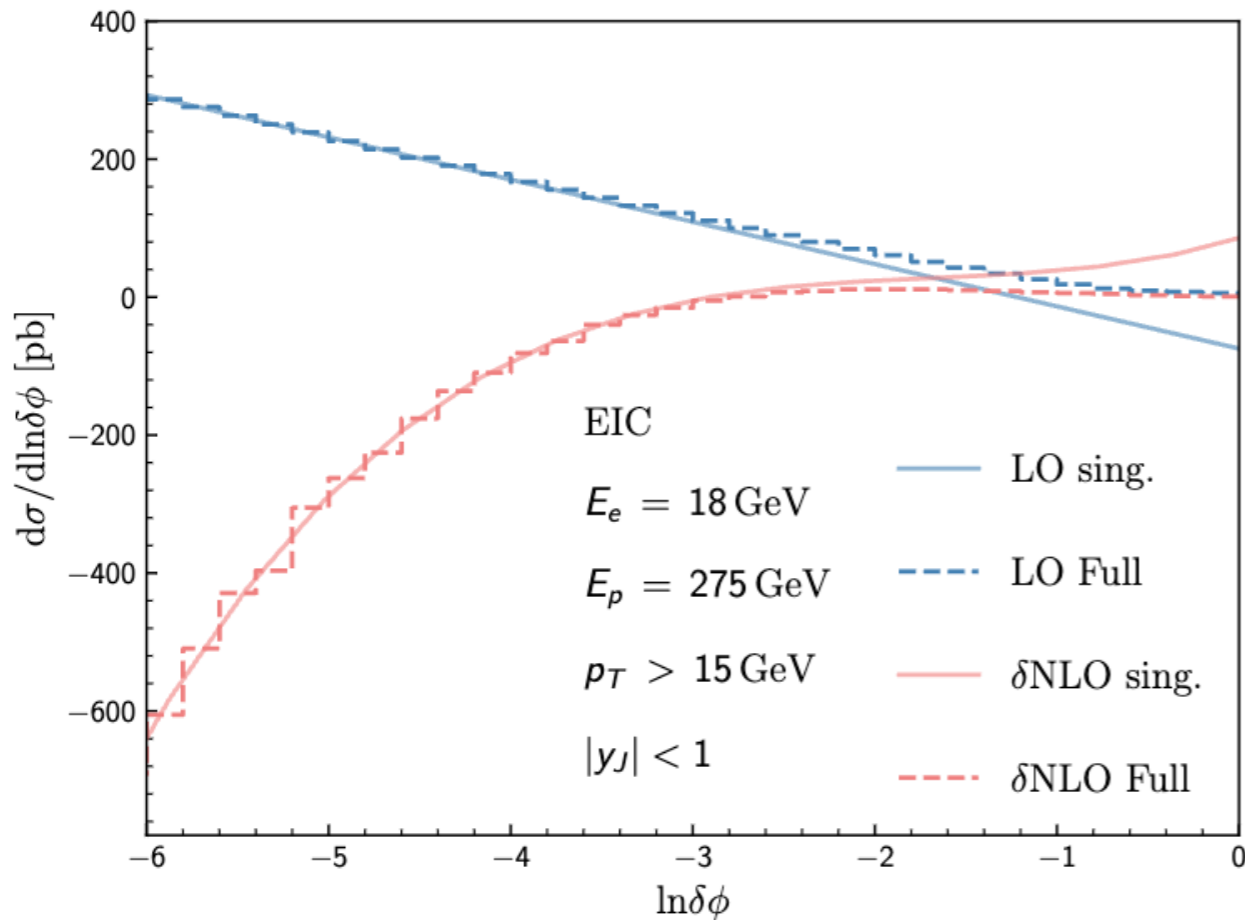
$$\begin{aligned}
 B = & C_F^2 \left[\frac{\bar{L}^4}{2} + 3\bar{L}^3 + \bar{L}^2 \left(\frac{11}{2} - \frac{\pi^2}{3} + 6 \ln 2 \right) + \bar{L} \left(\frac{9}{4} + 18 \ln 2 - 4 \zeta_3 \right) - \frac{189}{16} + 5 \pi^2 \right. \\
 & \left. - \frac{173 \pi^4}{720} + 27 \ln 2 - \frac{9}{2} \pi^2 \ln 2 + 9 \ln^2 2 - 3 \zeta_3 \right] + C_F C_A \left[\frac{11 \bar{L}^3}{9} + \bar{L}^2 \left(-\frac{35}{36} + \frac{\pi^2}{6} \right) \right. \\
 & \left. + \bar{L} \left(-\frac{57}{4} + \frac{11 \pi^2}{18} + 11 \ln 2 + 6 \zeta_3 \right) - \frac{51157}{1296} + \frac{1061 \pi^2}{216} - \frac{2 \pi^4}{45} + \frac{401 \zeta_3}{18} \right] \\
 & + C_F T_F n_f \left[-\frac{4 \bar{L}^3}{9} + \frac{\bar{L}^2}{9} + \bar{L} \left(5 - \frac{2 \pi^2}{9} - 4 \ln 2 \right) + \frac{4085}{324} - \frac{91 \pi^2}{54} - \frac{14 \zeta_3}{9} \right] \\
 & + \frac{j_2}{2},
 \end{aligned}$$



$N^3LL + \mathcal{O}(\alpha_s^2)$ predictions on lepton jet azimuthal correlation in DIS

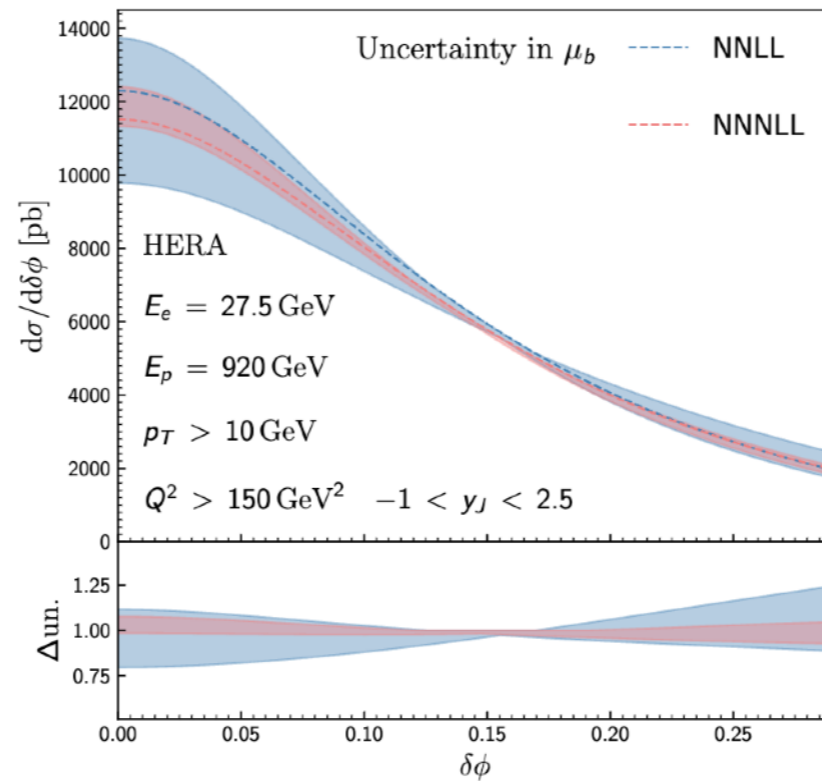
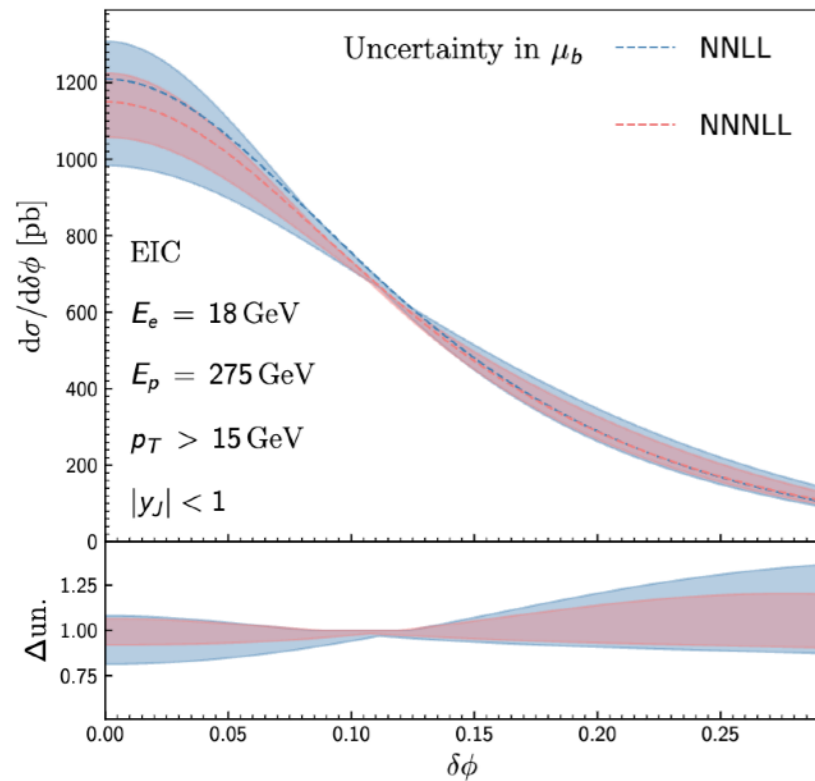
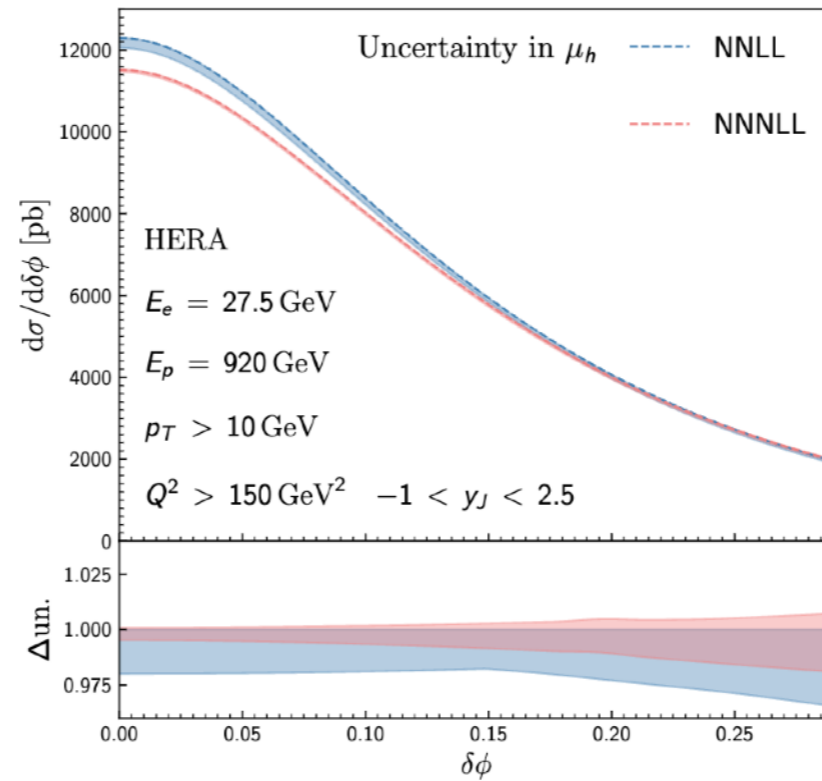
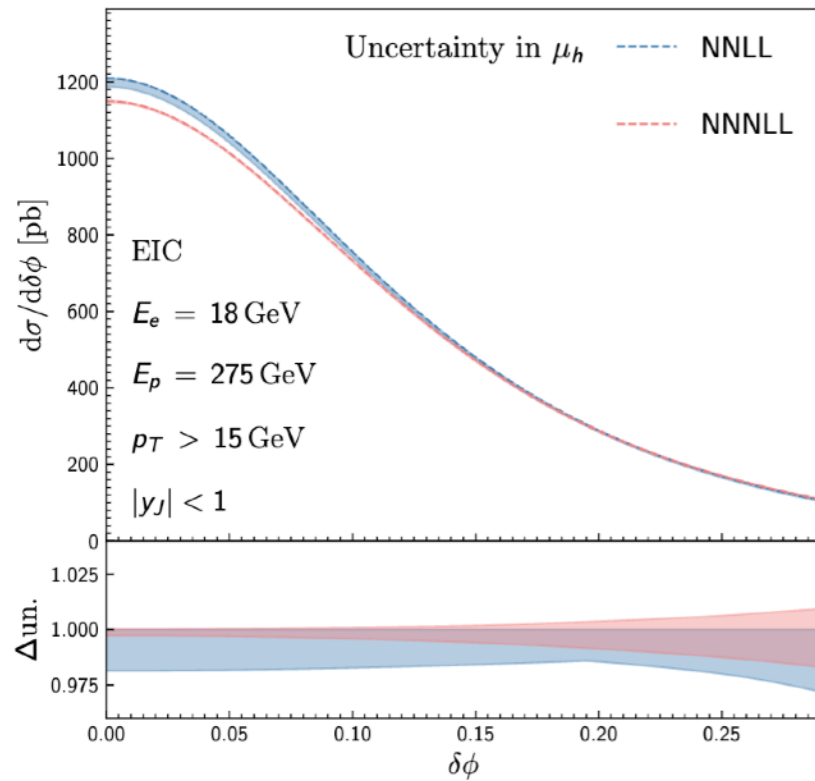
Fang, Gao, Li, DYS 2408.XXXXX

- We also compare the resummation expanded singular contribution in DIS with the full prediction from NLOJET++ up to $\mathcal{O}(\alpha_s^2)$.
- Good agreement in the back-to-back limit ($\delta\phi \rightarrow 0$) is observed.
- Matching corrections (Y term) are important in the large $\delta\phi$ region



Comparison of resummation results at N2LL and N3LL

Fang, Gao, Li, DYS 2408.XXXXX



- The uncertainty bands are narrower at N3LL (red) compared to NNLL (blue)

- At N3LL the dominant scale uncertainties are from μ_b variation

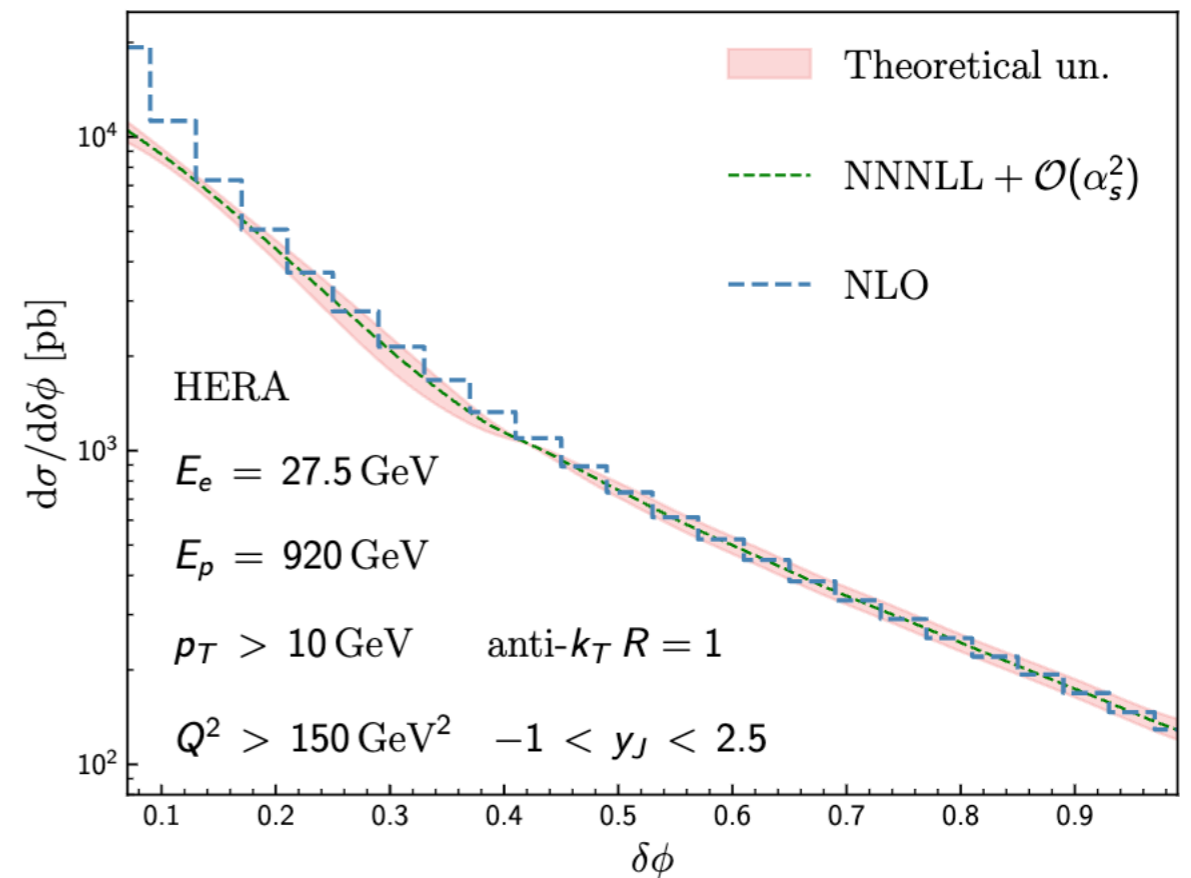
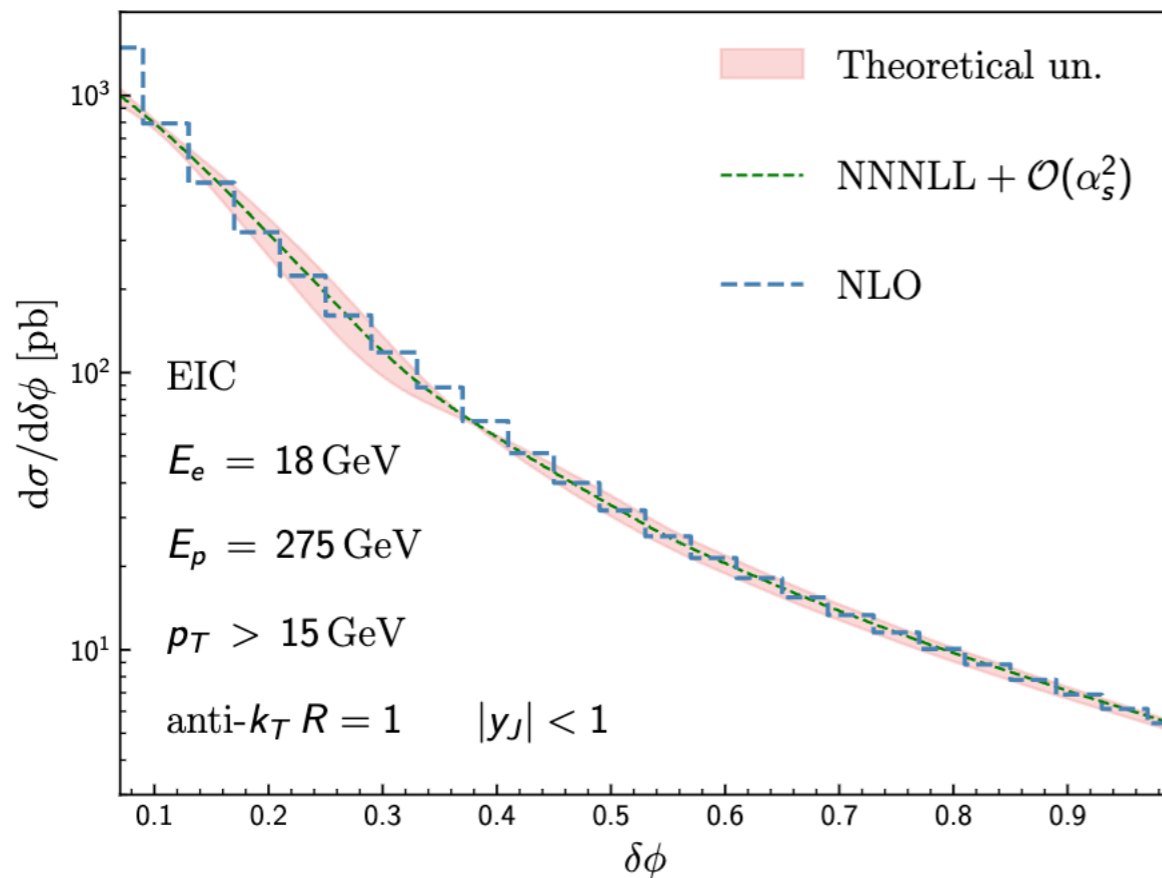
N³LL + $\mathcal{O}(\alpha_s^2)$ predictions on lepton jet azimuthal correlation in DIS

Fang, Gao, Li, DYS 2408.XXXXX

- In the large $\delta\phi$ region the resummation formula receives significant matching corrections
- It is necessary to switch off the resummation and instead employ fixed-order calculations

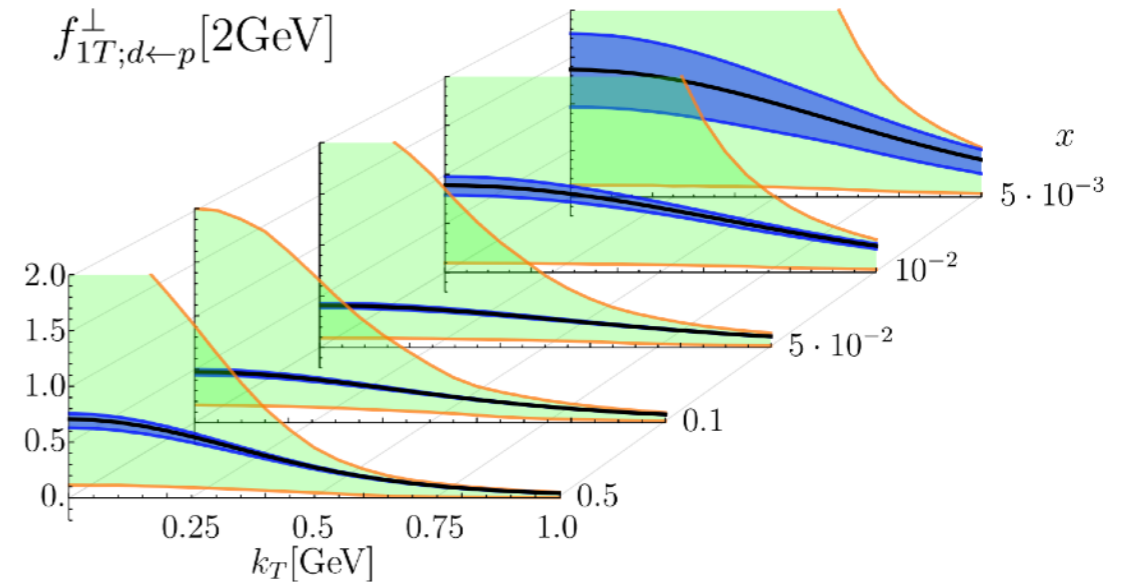
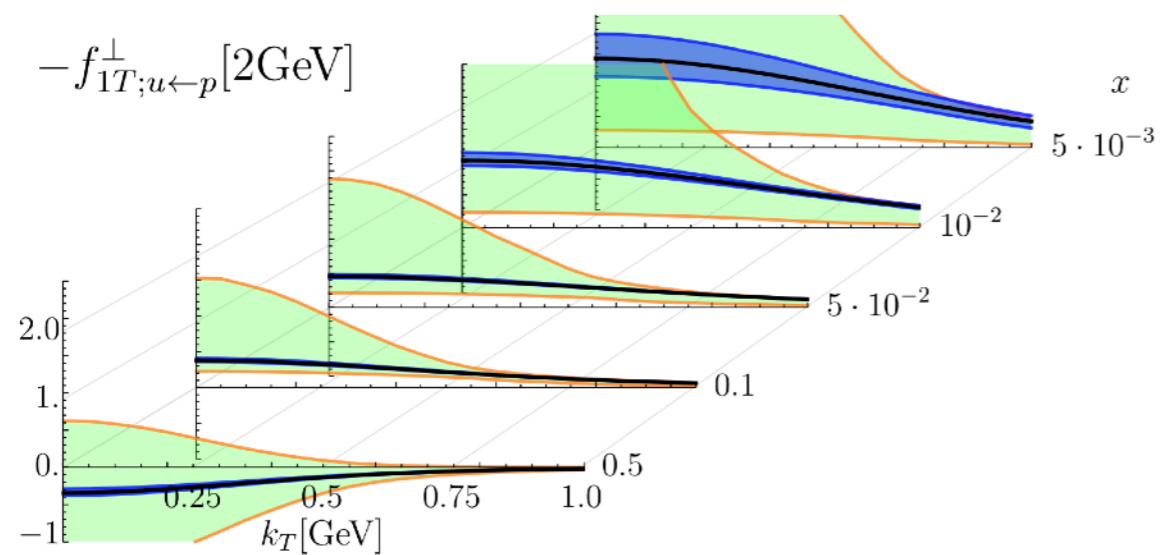
$$d\sigma_{\text{add}}(\text{NNNLL} + \mathcal{O}(\alpha_s^2)) \equiv d\sigma(\text{NNNLL}) + \underbrace{d\sigma(\text{NLO}) - d\sigma(\text{NLO singular})}_{d\sigma(\text{NLO non-singular})}$$

$$d\sigma(\text{NNNLL} + \mathcal{O}(\alpha_s^2)) = [1 - t(\delta\phi)]d\sigma_{\text{add}}(\text{NNNLL} + \mathcal{O}(\alpha_s^2)) + t(\delta\phi)d\sigma(\text{NLO})$$



TMDs in the large-x limit

Up and down quark Sivers distributions as a function of the transverse momentum k_T for different values of x



EIC Yellow report '21

How to give a reliable framework for extracting TMDs at large x value ?

TMDs in the large-x limit

- The usual TMD factorization is defined at moderate x value, i.e the x is not too low or too high
- TMDs at small x is important for gluon saturation in the Regge asymptotic of QCD, which was investigated in Balitsky, Tarasov '15, Zhou '16, Xiao, Yuan, Zhou '17

$$xG_{WW}(x, k_{\perp}, \zeta_c = \mu_F = Q) = -\frac{2}{\alpha_S} \int \frac{d^2v_{\perp} d^2v'_{\perp}}{(2\pi)^4} e^{ik_{\perp} \cdot r_{\perp}} \mathcal{H}^{WW}(\alpha_S(Q)) e^{-S_{sud}(Q^2, r_{\perp}^2)} \mathcal{F}_{Y=\ln 1/x}^{WW}(v_{\perp}, v'_{\perp})$$

- In the limit $x \rightarrow 1$ (threshold), the phase space of real radiations is restricted

E.g. : One-loop quark TMDs in the parton model

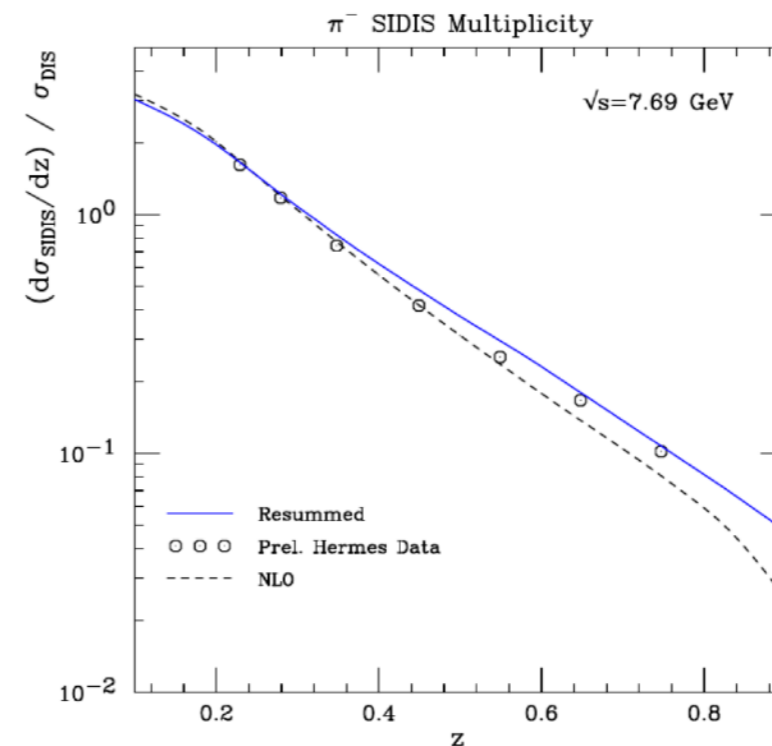
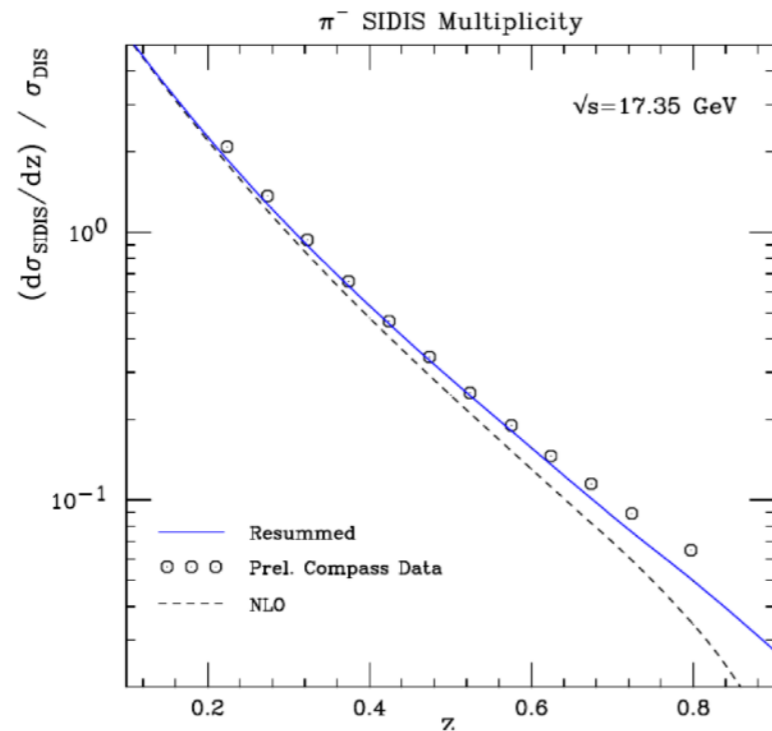
$$\tilde{f}_{q/q}^{(1)}(x, \mathbf{b}_T, \mu, \zeta) = \frac{\alpha_S(\mu) C_F}{2\pi} \left[-\left(\frac{1}{\epsilon} + L_b\right) [P_{qq}(x)]_+ + (1-x) - \frac{L_b^2}{2} + L_b \left(\frac{3}{2} + \ln \frac{\mu^2}{\zeta}\right) - \frac{\pi^2}{12} \right]$$

$$P_{qq}(x) = \frac{1+x^2}{1-x}$$

divergent as $x \rightarrow 1$

Threshold resummation

- The threshold effect is important for a reliable theoretical prediction near the right edge of the phase space, e.g. threshold resummation of pion FFs [Anderle, Ringer, Vogelsang '13](#)



- The NLL joint resummation framework of threshold and TMD logarithms was first developed by [Laenen, Sterman & Vogelsang '00](#) ...
- A factorization formula based on SCET then was given by [Lustermans, Waalewijn, Zeune '16](#) . [Y. Li, Neill, Zhu '16](#)
- We apply the joint threshold and TMD factorization theorem to introduce new threshold-TMDs — **TTMDs** [Kang, Samanta, Shao, Zeng '22 JHEP](#)

From TMDs to TTMDs

- Consider Drell-Yan process

$$h_1(P_1) + h_2(P_2) \rightarrow \gamma^*(q) \rightarrow l^+ + l^- + X$$

- As $q_T \ll Q$, we have the TMD factorization theorem

$$\frac{d^3\sigma^{\text{DY}}}{d^2\mathbf{q}_T d\tau^{\text{DY}}} = \sigma_0^{\text{DY}} \int_{C_N} \frac{dN}{2\pi i} (\tau^{\text{DY}})^{-N} \int \frac{d^2\mathbf{b}_T}{4\pi^2} e^{i\mathbf{q}_T \cdot \mathbf{b}_T} H^{\text{DY}}(Q, \mu) \sum_q e_q^2 \tilde{f}_{q/h_1}^{\text{TMD}}(N, b_T, \mu, \zeta) \tilde{f}_{\bar{q}/h_2}^{\text{TMD}}(N, b_T, \mu, \zeta)$$

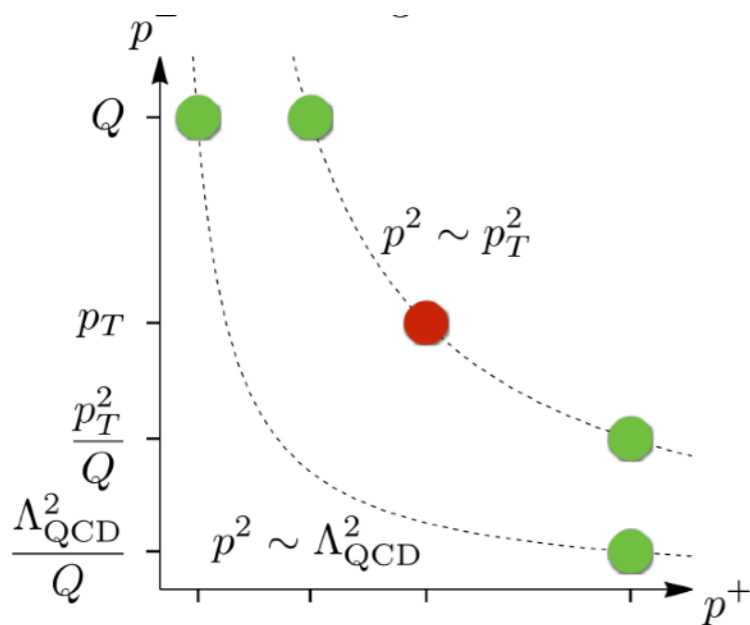
- **Threshold variables:** $\tau^{\text{DY}} \equiv Q^2/S$ $\hat{\tau}^{\text{DY}} \equiv \tau^{\text{DY}}/(x_1 x_2)$
- **TMDPDFs after Mellin transformation:** $\tilde{f}_{i/h}^{\text{TMD}}(N, b_T, \mu, \zeta) \equiv \int_0^1 dx x^{N-1} f_{i/h}^{\text{TMD}}(x, b_T, \mu, \zeta)$
- **When the partonic threshold variable is close to 1, i.e. $N \rightarrow \infty$, the above factorization is not complete**
- **To include both the TMD and threshold effects, we perform a re-factorization for the TMDPDF**

$$\tilde{f}_{i/h}^{\text{TMD}}(N, b_T, \mu, \zeta) \xrightarrow{N \rightarrow \infty} \tilde{S}_c(N, b_T, \mu, \zeta) \tilde{f}_{i/h}(N, \mu)$$

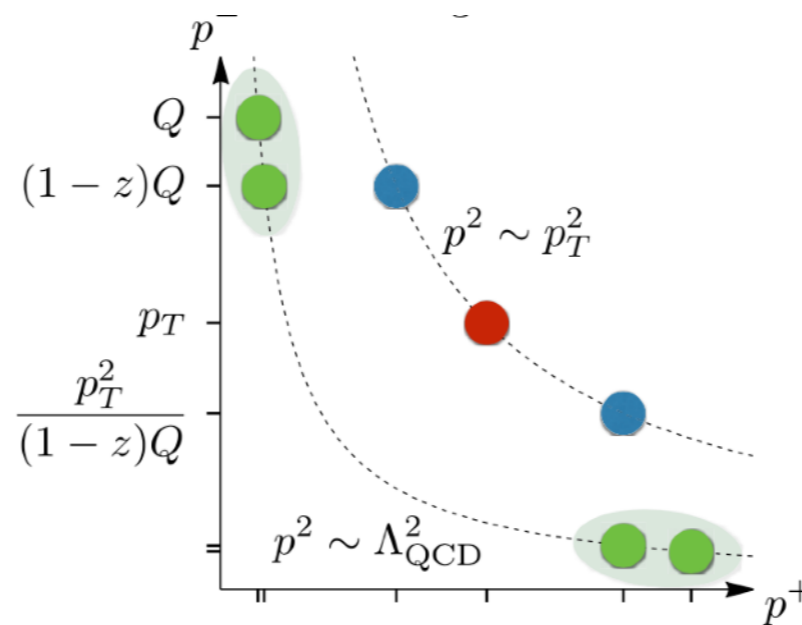
EFT in the joint limit

In the threshold limit, the new scale hierarchy introduces an additional degrees of freedom known as collinear-soft degrees of freedom

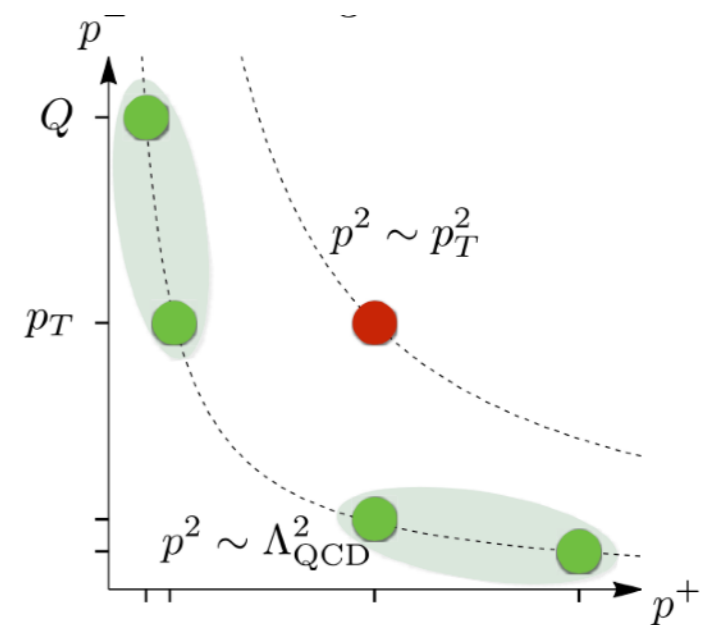
$$k_{cs}^\mu \equiv (\bar{n} \cdot k_{cs}, n \cdot k_{cs}, k_{cs,\perp}) \sim \left(Q(1 - \hat{\tau}), \frac{q_T^2}{Q(1 - \hat{\tau})}, q_T \right)$$



$$Q \sim (1 - z)Q \gg p_T$$



$$Q \gg (1 - z)Q \gg p_T$$



$$Q \gg (1 - z)Q \sim p_T$$

TMD soft function is the same as usual, so the rapidity div. is not changed

Collinear-soft function

In the threshold limit, the new scale hierarchy introduces an additional degrees of freedom known as collinear-soft degrees of freedom

To validate the factorization theorem, we employ the threshold expressions of the perturbative matching coefficients to ascertain the **three-loop collinear-soft function**.

$$\tilde{S}_c^{(1)} = 2C_F L_b L_\zeta,$$

$$\begin{aligned} \tilde{S}_c^{(2)} = & 2C_F^2 L_b^2 L_\zeta^2 + C_F C_A \left[\frac{11}{3} L_b^2 + \left(\frac{134}{9} - 4\zeta_2 \right) L_b + \left(\frac{404}{27} - 14\zeta_3 \right) \right] L_\zeta \\ & + C_F T_F n_f \left(-\frac{4}{3} L_b^2 - \frac{40}{9} L_b - \frac{112}{27} \right) L_\zeta, \end{aligned}$$

$$\begin{aligned} \tilde{S}_c^{(3)} = & \frac{4}{3} C_F^3 L_b^3 L_\zeta^3 + C_F^2 C_A \left[\frac{22}{3} L_b^3 + \left(\frac{268}{9} - 8\zeta_2 \right) L_b^2 + \left(\frac{808}{27} - 28\zeta_3 \right) L_b \right] L_\zeta^2 \\ & + C_F C_A^2 \left[\frac{242}{27} L_b^3 + \left(\frac{1780}{27} - \frac{44}{3} \zeta_2 \right) L_b^2 + \left(\frac{15503}{81} - \frac{536}{9} \zeta_2 - 88\zeta_3 + 44\zeta_4 \right) L_b \right. \\ & \left. + \left(\frac{297029}{1458} - \frac{3196}{81} \zeta_2 - \frac{6164}{27} \zeta_3 + \frac{88}{3} \zeta_2 \zeta_3 - \frac{77}{3} \zeta_4 + 96\zeta_5 \right) \right] L_\zeta \\ & + C_F C_A T_F n_f \left[-\frac{176}{27} L_b^3 + \left(-\frac{1156}{27} + \frac{16}{3} \zeta_2 \right) L_b^2 + \left(-\frac{8204}{81} + \frac{160}{9} \zeta_2 \right) L_b \right. \\ & \left. + \left(-\frac{62626}{729} + \frac{824}{81} \zeta_2 + \frac{904}{27} \zeta_3 - \frac{20}{3} \zeta_4 \right) \right] L_\zeta \\ & + C_F T_F^2 n_f^2 \left(\frac{32}{27} L_b^3 + \frac{160}{27} L_b^2 + \frac{800}{81} L_b + \frac{3712}{729} + \frac{64}{9} \zeta_3 \right) L_\zeta \\ & + C_F^2 T_F n_f \left[-\frac{8}{3} L_b^3 L_\zeta^2 + \left(-4 - \frac{80}{9} L_\zeta \right) L_b^2 L_\zeta + \left(-\frac{224}{27} - \frac{110}{3} + 32\zeta_3 \right) L_b L_\zeta^2 \right. \\ & \left. + \left(-\frac{1711}{27} + \frac{304}{9} \zeta_3 + 16\zeta_4 \right) L_\zeta \right], \end{aligned}$$

Collins-Soper scale in the joint limit

The Collins-Soper equation is the same as the one for TMD PDFs

$$\tilde{S}_c(N, b_T, \mu_b, \zeta_f) = \tilde{S}_c(N, b_T, \mu_b, \zeta_i) \left(\sqrt{\frac{\zeta_f}{\zeta_i}} \right)^{\kappa(b_T, \mu_b)}$$

where $\zeta_i = \mu_b^2 = b_0^2/b_T^2$ and ζ_f is determined from RG consistency

RG equations for the hard function, collinear-soft function and collinear PDFs read

$$\begin{aligned} \mu \frac{d}{d\mu} H^{\text{DY}}(Q, \mu) &= \Gamma^h(\alpha_s) H^{\text{DY}}(Q, \mu), \\ \mu \frac{d}{d\mu} \tilde{S}_c(N, b_T, \mu, \zeta_f) &= \Gamma^{\tilde{S}_c}(\alpha_s, \zeta_f) \tilde{S}_c(N, b_T, \mu, \zeta_f), \\ \mu \frac{d}{d\mu} \tilde{f}_q(N, \mu) &= \Gamma^{\tilde{f}_q}(\alpha_s) \tilde{f}_q(N, \mu), \end{aligned}$$

with

$$\begin{aligned} \Gamma^h(\alpha_s) &= 2 \Gamma_{\text{cusp}}(\alpha_s) \ln \frac{Q^2}{\mu^2} + 2\gamma_V(\alpha_s), \\ \Gamma^{\tilde{S}_c}(\alpha_s, \zeta_f) &= -\Gamma_{\text{cusp}}(\alpha_s) \ln \frac{\zeta_f}{\mu^2} + \gamma_{\tilde{S}_c}(\alpha_s), \\ \Gamma^{\tilde{f}_q}(\alpha_s) &= -2 \Gamma_{\text{cusp}}(\alpha_s) \ln \bar{N} + 2\gamma_{\tilde{f}_q}(\alpha_s), \end{aligned}$$

We find the Collins-Soper scale in the threshold limit is given by $\zeta_f^{\text{TTMD}} = \frac{Q^2}{\bar{N}^2} \sim Q^2(1 - \hat{\tau})^2$

which is different from the standard TMD one $\zeta_f^{\text{TMD}} = Q^2$

Threshold-TMDPDF

After solving RG evolution and CS evolution, we have TTMDPDF

$$\tilde{f}_{i/h}^{\text{TTMD}}(N, b_T, Q) = \exp \left[-S_{\text{pert}}(Q, \mu_{b_*}, \mu_F) - S_{\text{NP}}^f(b_T, Q_0, \zeta_f^{\text{TTMD}}) \right] \tilde{f}_{i/h}(N, \mu_F)$$

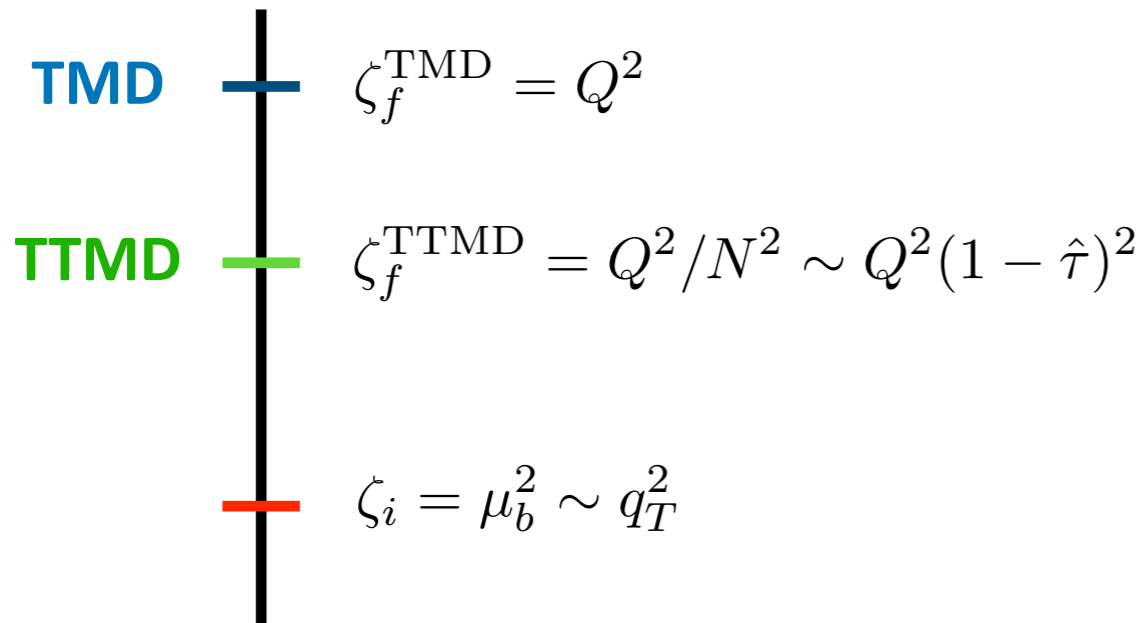
where the function form of the perturbative Sudakov factor and non-perturbative parts are the same as the usual TMD ones, but the CS scale is modified

For large value of N, the Collins-Soper scale may go down the non-perturbative region, so we introduce a prescription to freeze the value of CS scale

$$\zeta_* \equiv \zeta_*(\zeta_f^{\text{TTMD}}, Q_0) = \left(\frac{Q}{\bar{N}} \right)^2 \left(1 + \frac{Q_0^2 \bar{N}^2}{Q^2} \right)$$

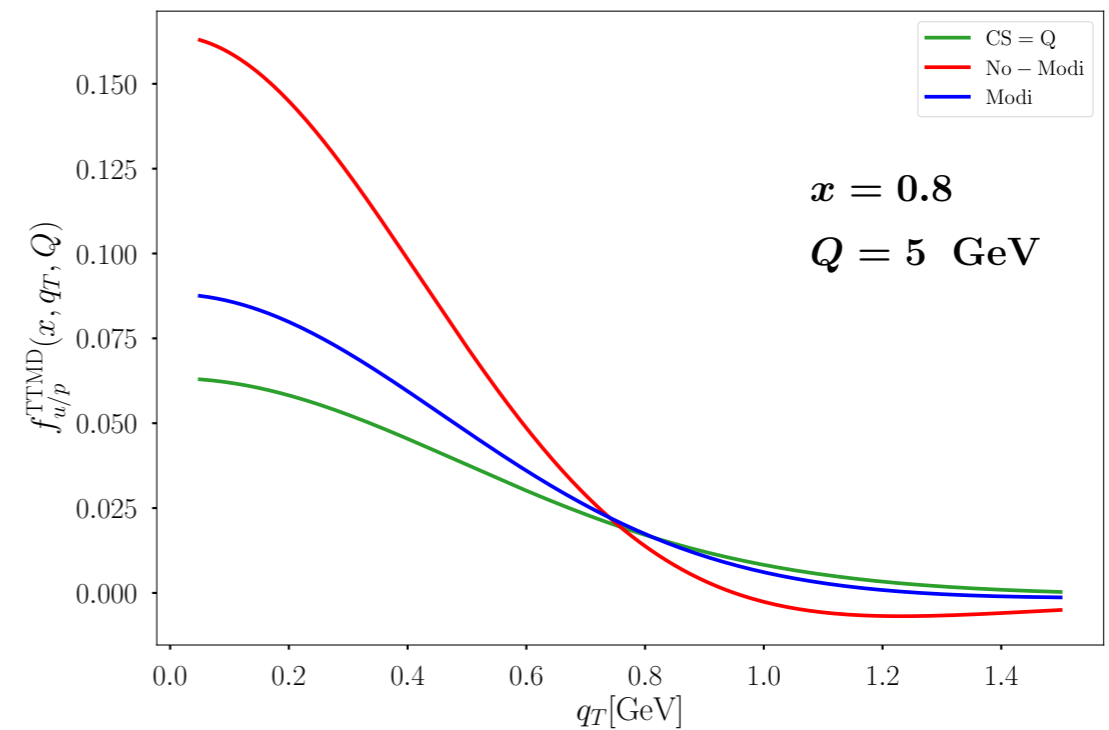
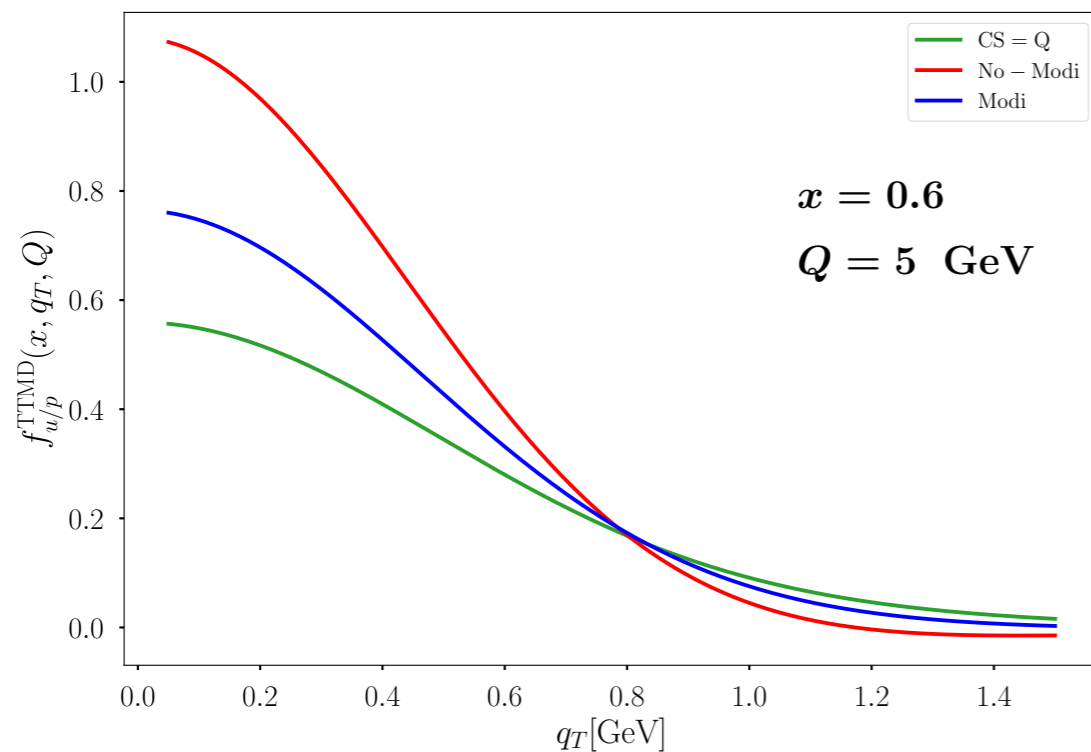
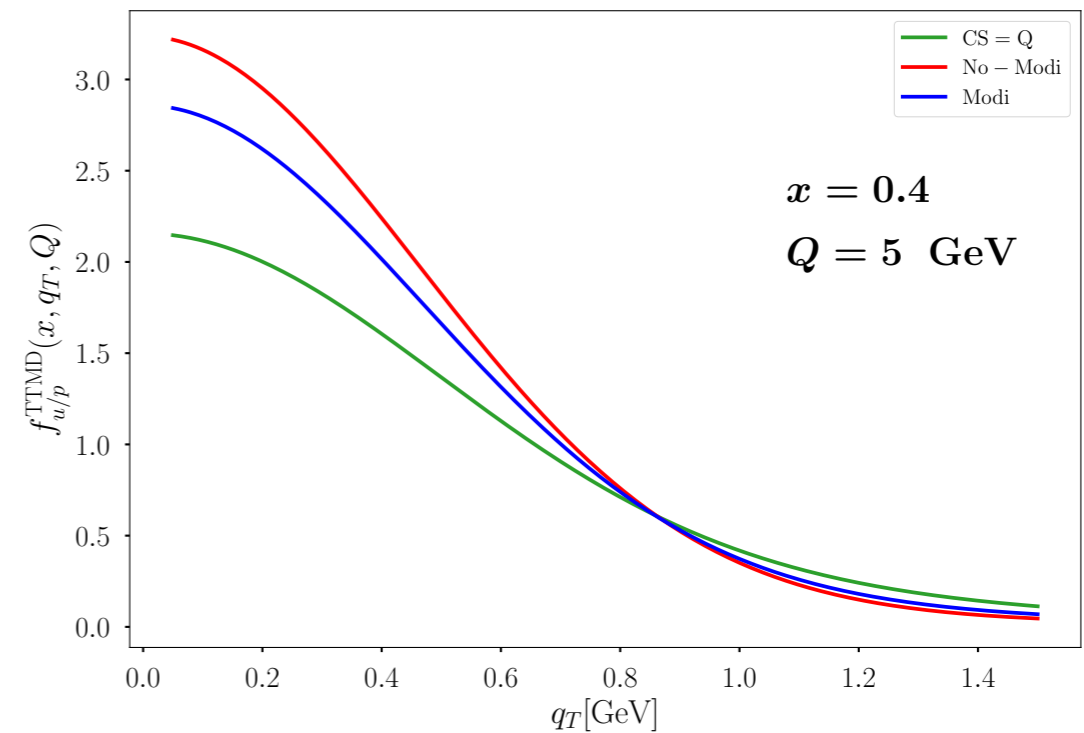
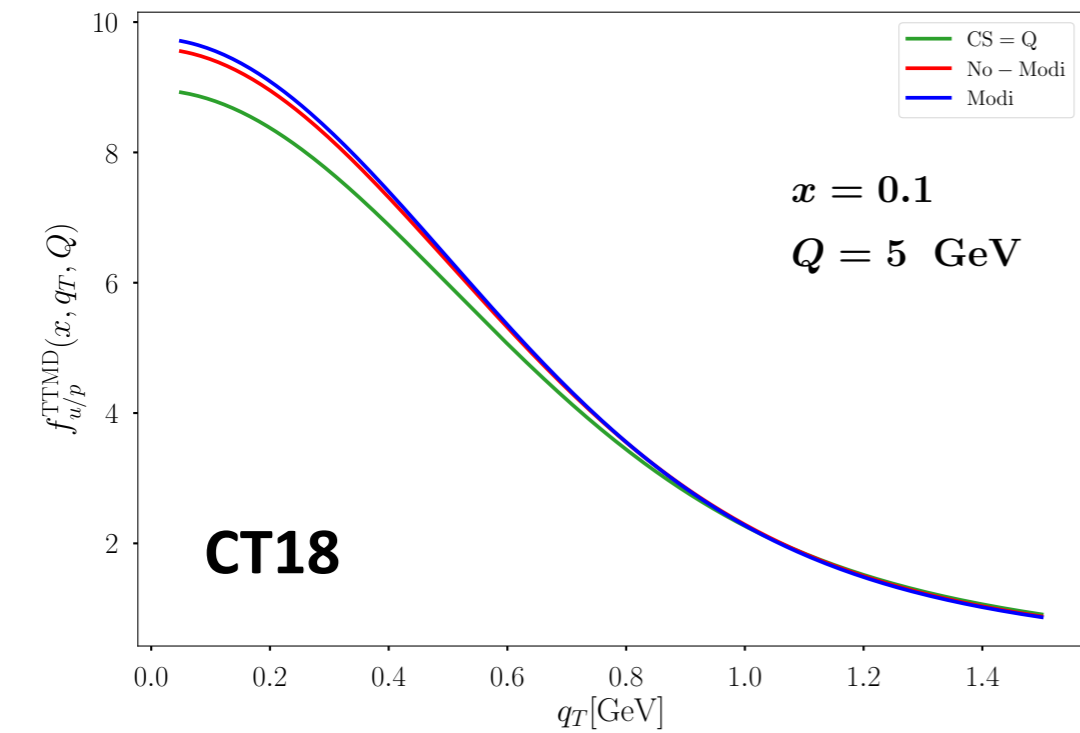
where Q_0 is given in the NP Sudakov

$$S_{\text{NP}}(b_T, Q_0, \zeta_f) = g_1^f b_T^2 + \frac{g_2}{2} \ln \frac{\sqrt{\zeta_f}}{Q_0} \ln \frac{b_T}{b_*}$$

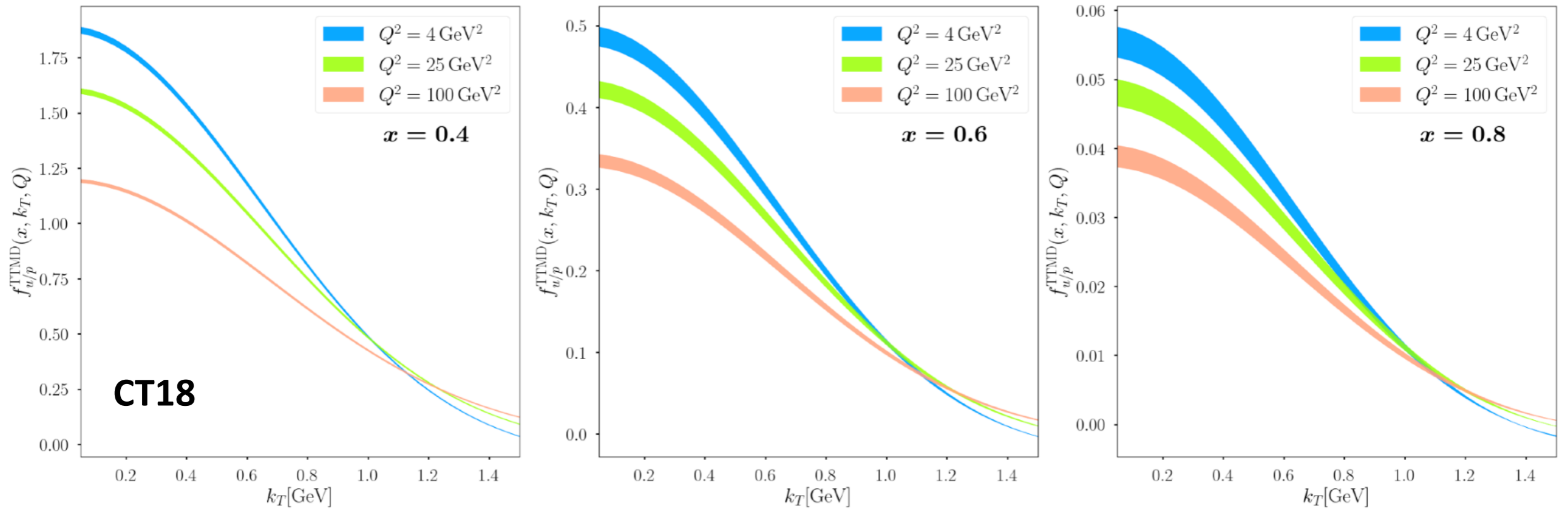


Numerical results for threshold-TMDPDF

TMD TTMD TTMD (ζ_* -prescription)



Numerical results for threshold-TMDPDFs



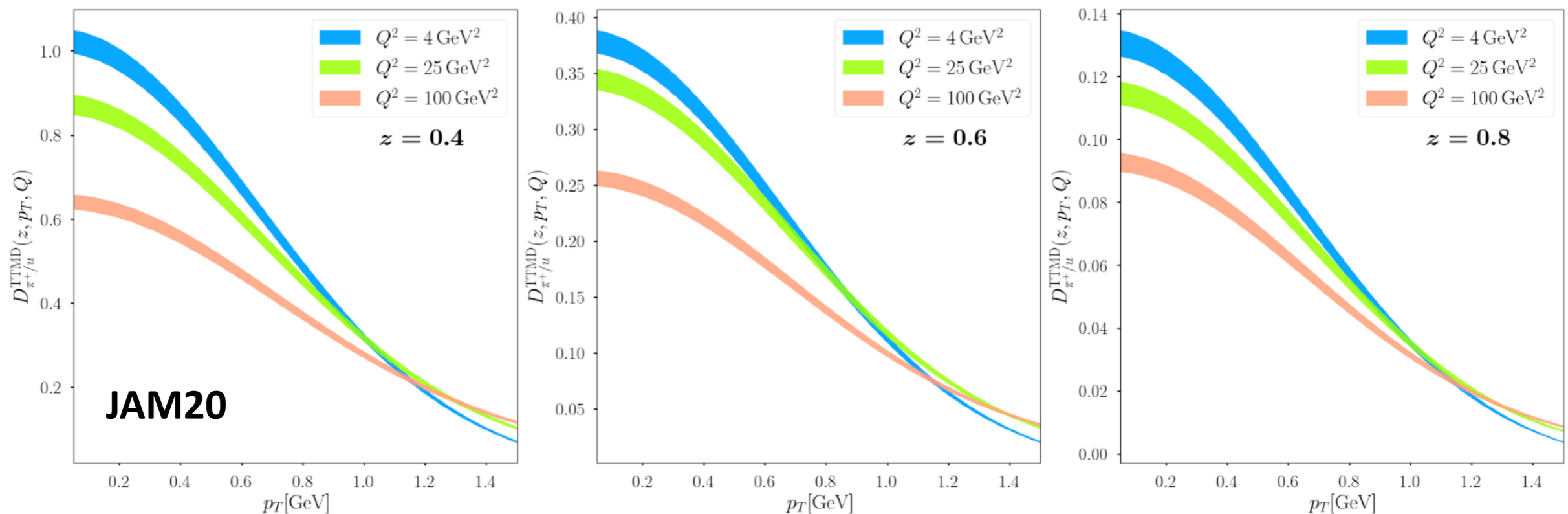
The uncertainty bands correspond to the $1-\sigma$ variation from CT18 PDFs using the Hessian method

Threshold-TMDFFs

We show the universality of threshold-TMD functions among three standard processes, i.e. the Drell-Yan production in pp collisions, semi-inclusive deep-inelastic scattering and back-to-back two hadron production in e^+e^- collisions

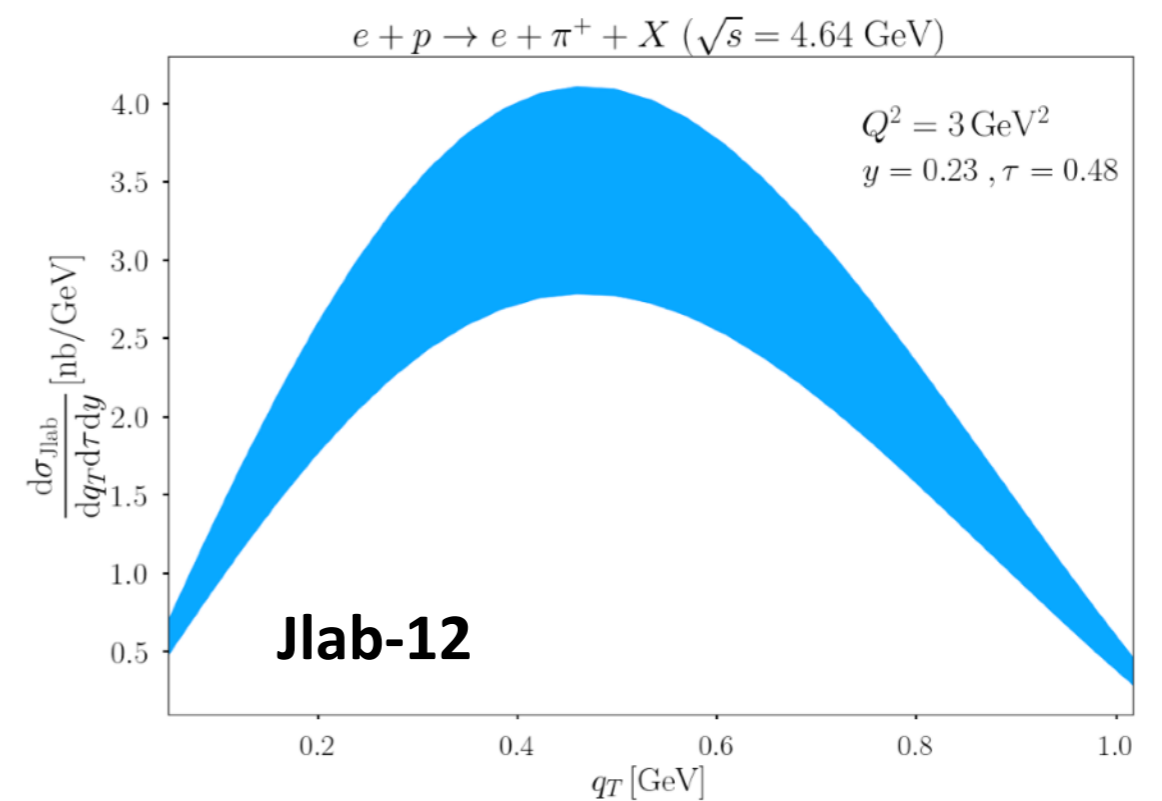
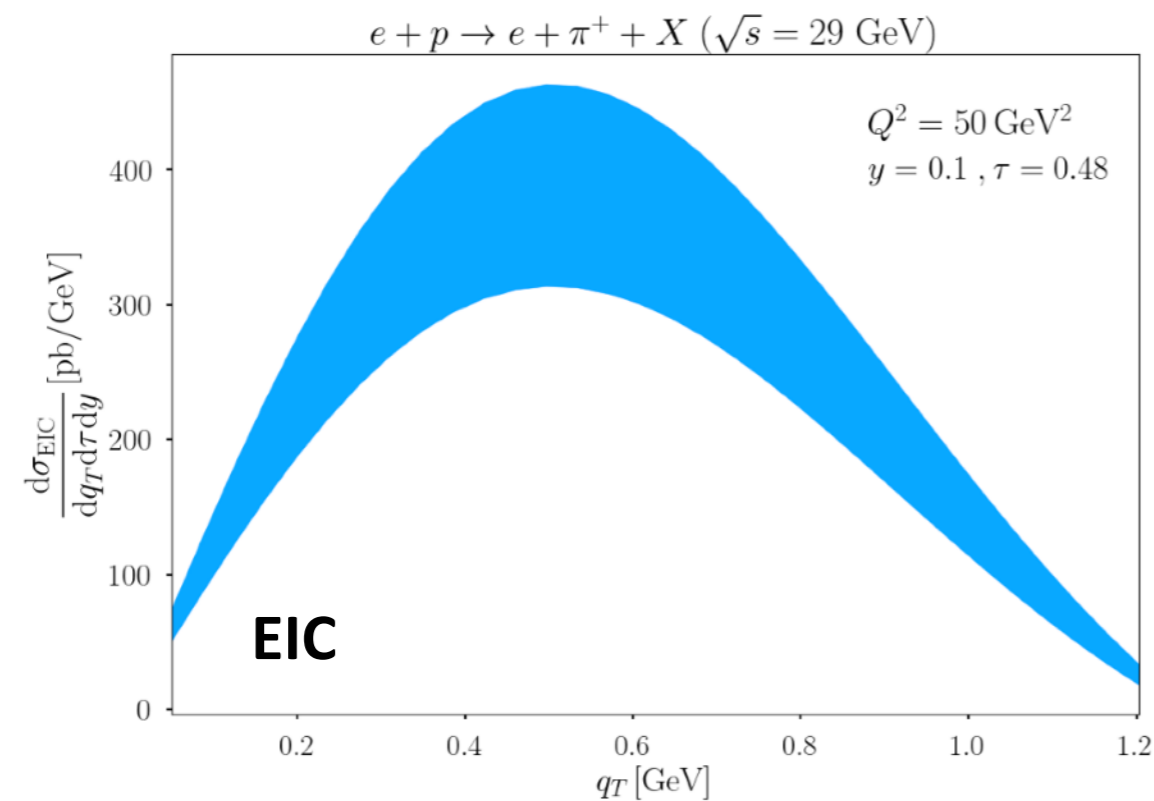
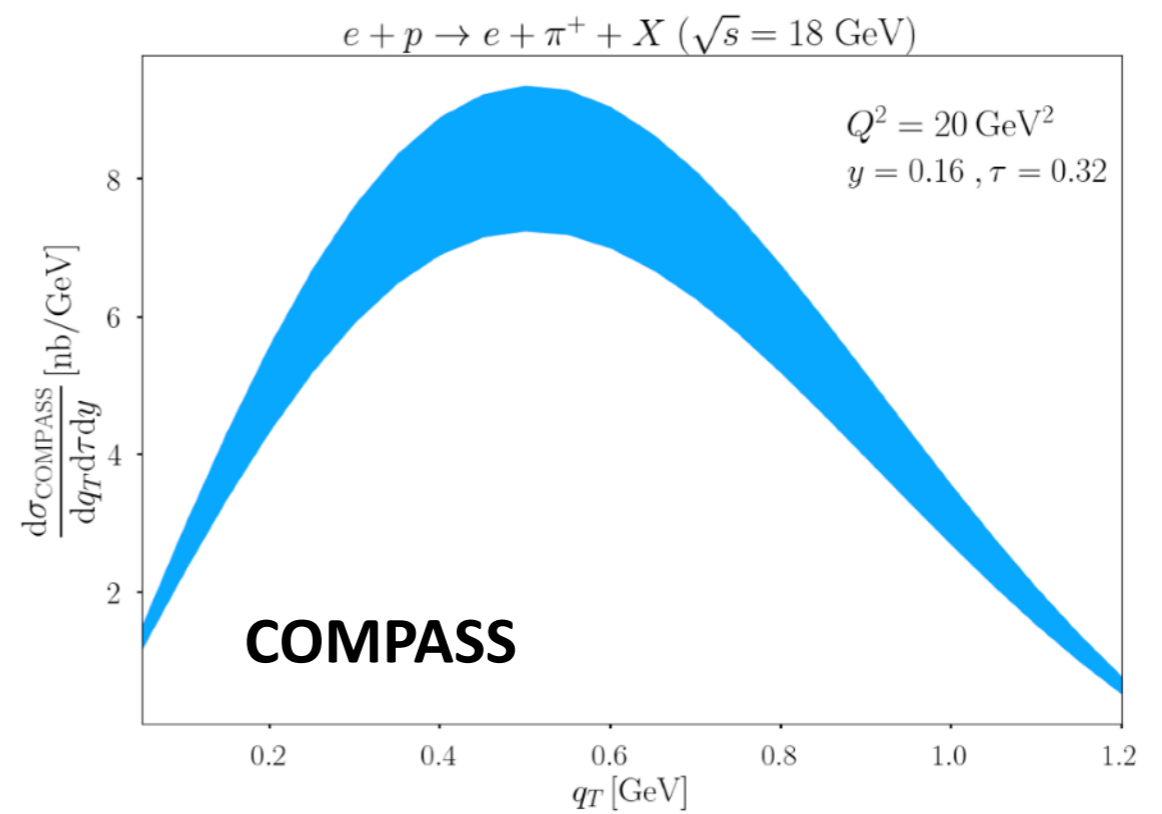
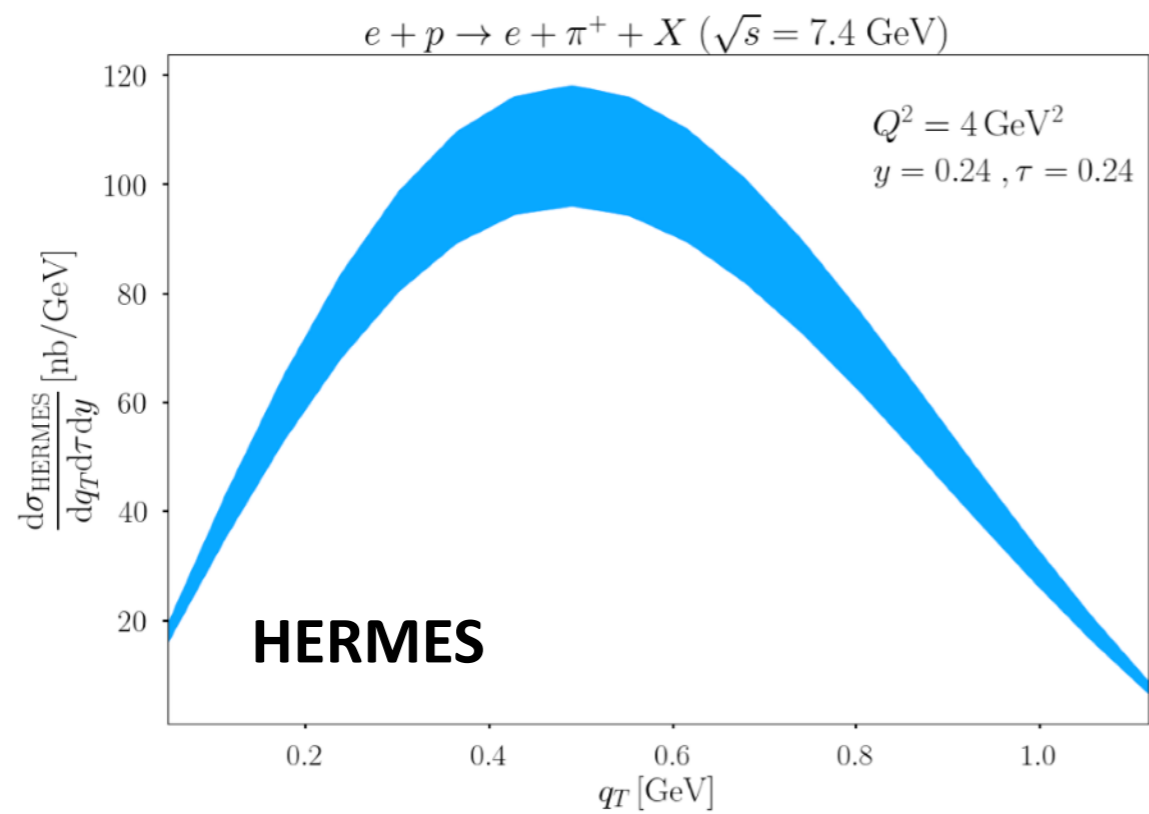
$$f_{q/p}^{\text{TTMD}}(x, \mathbf{k}_T, Q)|_{\text{SIDIS}} = f_{q/p}^{\text{TTMD}}(x, \mathbf{k}_T, Q)|_{\text{DY}},$$

$$D_{h/q}^{\text{TTMD}}(z, \mathbf{p}_T, Q)|_{\text{SIDIS}} = D_{h/q}^{\text{TTMD}}(z, \mathbf{p}_T, Q)|_{e^+e^-}.$$



The uncertainty bands correspond to $1-\sigma$ variation of JAM FFs using the replica method.

Cross section for SIDIS



Summary and outlook

We provide a theoretical formalism for the threshold improved TMDs

In our analysis, we observe that to have a kinematic consistence result, one needs to modify Collins-Soper scale $\zeta_f^{\text{TMD}} = Q^2/N^2 \sim Q^2(1 - \hat{\tau})^2$

We introduce a new ζ_* -prescription to freeze the CS scale

Our formalism will serve as a reliable theoretical input for extracting the TMD functions at large x value

Future experimental analysis and global fitting analysis will help in unveiling the three-dimensional picture of a hadron in the large x limit

The corresponding theoretical predictions on the spin asymmetry in the threshold limit will be explored in future work

Thank you